RBRH

Revista Brasileira de Recursos Hídricos
Brazilian Journal of Water Resources
Versão On-line ISSN 2318-0331
RBRH, Porto Alegre, v. 29, e24, 2024
Scientific/Technical Article

https://doi.org/10.1590/2318-0331.292420230134

Study of the influence of the Tebessa region wastewaters on the hydrochemical quality of the alluvial aquifer groundwater's Tebessa-Ain Chabro (N-E Algeria)

Estudo da influência das águas residuais da região de Tebessa na qualidade hidroquímica das águas subterrâneas do aquífero aluvial de Tebessa-Ain Chabro (Nordeste da Argélia)

Messaoud Abidi Saad[1], Karima Seghir[1], Abdeldjebar Touahri[2], Mehdi Bendekkoum[1], Abdelaziz Bellaoueur[2] & Antonio Pulido-Bosch[3]

[1]Echahid Cheikh Larbi Tébessi University, Tébessa, Algeria
[2]Kasdi Merbah Ouargla University, Ouargla, Algeria
[3]University of Granada, Granada, Spain

E-mails: messaoud.abidisaad@univ-tebessa.dz (MAS), Karima.seghir@univ-tebessa.dz (KS), touahriaaljebar@gmail.com (AT), mehdi.bendekkoum@univ-tebessa.dz (MB), bellaoueuraz@gmail.com (AB), apulido@ual.es (APB)

Received: November 20, 2023 - Revised: April 22, 2024 - Accepted: May 09, 2024

ABSTRACT

Along the Algerian-Tunisian border in northeastern Algeria, groundwater is regarded as the primary source of agricultural and drinking water for the local community. This situation is the result of low rainfall and limited surface water. Finding out how wastewater discharges affect the physicochemical and bacteriological quality of alluvial groundwater is the objective of this research paper. Thirty-six wells and boreholes were targeted to collect water samples. The analysis results show that the waters ranged from acidic to neutral ($6.46 \leq pH \leq 8.3$), and moderately to highly mineralized ($754\ \mu S/cm < C.E < 11680\ \mu S/cm$). The main water types, according to the Piper diagram, are calcic bicarbonate ($HCO_3^-\ Ca^{2+}$) and calcic chloride ($Cl^-\ Ca^{2+}$). Total coliforms and *Escherichia Coli* were detected in 60 and 100% of the water samples analyzed, respectively. The geospatial data shows that the chemical and bacteriological pollution progresses from upstream to downstream, from Oued El Kebir river in the South East to Oued Chabro River in the North West. The multivariable statistical analysis (Principal Component Analysis and Closer Analysis) highlighted that water mineralization is controlled by three major phenomena, which are water-rock hydrolysis interaction, leaching of geological formations, and influence of anthropogenic activities.

Keywords: Algeria; Groundwater; Pollution; Wastewater; Bacteriological; Statistical analysis.

RESUMO

Ao longo da fronteira entre a Argélia e a Tunísia, no nordeste do país, as águas subterrâneas são consideradas a principal fonte de água potável e agrícola para a comunidade local. Essa situação é resultado da baixa pluviosidade e da limitação das águas superficiais. O objetivo deste trabalho de pesquisa é descobrir como as descargas de águas residuais afetam a qualidade físico-química e bacteriológica das águas subterrâneas aluviais. Trinta e seis poços e boreholes foram utilizados para coletar amostras de água. Os resultados da análise mostram que as águas variaram de ácidas a neutras ($6{,}46 \leq pH \leq 8{,}3$) e de moderadamente a altamente mineralizadas ($754\ \mu S/cm < C.E < 11680\ \mu S/cm$). Os principais tipos de água, de acordo com o diagrama de Piper, são bicarbonato cálcico ($HCO_3^-\ Ca^{2+}$) e cloreto cálcico ($Cl^-\ Ca^{2+}$). Coliformes totais e *Escherichia Coli* foram detectados em 60 e 100% das amostras de água analisadas, respectivamente. Os dados geoespaciais mostram que a poluição química e bacteriológica progride de montante para jusante, do rio Oued El Kebir, no sudeste, até o rio Oued Chabro, no noroeste. A análise estatística multivariável (análise de componentes principais e análise de aproximação) destacou que a mineralização da água é controlada por três fenômenos principais, que são a interação hidrólise da água-rocha, a lixiviação de formações geológicas e a influência de atividades antropogênicas.

Palavras-chave: Algéria; Águas subterrâneas; Poluição; Águas residuais; Bacteriológicas; Análise estatística.

INTRODUCTION

Algeria is rapidly becoming a more urbanized country; between 2000 and 2020, the country's population increased from 31.1 to 44.3 million, and its annual trash output in landfills ranged from 10.9 to 13.6 million tons. As a result, the need for landfills in the country's major cities increased (Brahmi et al., 2021). The city of Tebessa shows rapid urbanization and industrial development, resulting in a very high-water demand for human consumption or industry. This development is accompanied by an increase in the flow of discharged wastewater and the degree of pollution of surface water and groundwater, with large quantities of wastewater untreated (urban and industrial).

In arid and semi-arid regions, the shallow depth of groundwater, combined with the influence of climatic conditions, significantly exacerbates its susceptibility to pollution. In 2020, the population estimate was 794528 population (Toumi & Alkama, 2022), there will unavoidably be a significant rise in the demand for water due to this population growth (Naimi-Ait-Aoudia & Berezowska-Azzag, 2014), a single sewage treatment plant - STP - located in Ain Chabro but does in it's full operation due to the lack of wastewater transport pipes. This wastewater is discharged directly into the El Kebir and Chabro rivers, that posing a perpetual threat of water resource degradation. The Tebessa region experiences a typical semi-arid continental climate, with cold winters and hot summers and an average annual temperature of 16 °C. The region receives approximately 370 mm of precipitation on average per year (Fehdi et al., 2016), of which 332.5 mm is estimated to be actual evapotranspiration, accounting for about 90% of the precipitation. Several factors that affect the chemical composition of the aquifer, such as lithology, temperature, pH, and the amount of water available in the aquifer, as well as climatic conditions, all contribute to the degradation of groundwater quality (L et al., 2015). In addition to those natural factors, anthropogenic activities have the primary role in the degradation of the groundwater characteristics. The situation has gotten worse due to the usage of pesticides and fertilizers in agricultural activities as well as the disposal of agricultural, animal, and human waste. (Annapoorna & Janardhana, 2015; Brahmi et al., 2021; Chakraborty et al., 2022; Modibo Sidibé et al., 2019). Groundwater supplies in the studied area are declining both qualitatively and quantitatively due to anthropogenic restrictions (drawing much more than the present recharge) and environmental limitations (typically an arid climate and rainfall volatility) (Fehdi et al., 2016; Rouabhia et al., 2009; Seghir, 2014). The Wadis of El Kebir and Chabro, which have an erratic flow regime due to the extended dry season, effectively drain this area of the Merja plane. The salinity of the water varies considerably; in certain places (the eastern portion of the research area), it surpasses 5 g/L. Several studies have been conducted regarding the alluvial aquifer of Tebessa (Drias & Toubal, 2015; Fehdi et al., 2016; Rouabhia et al., 2009; Seghir, 2014). However, the incorporation of pollutant parameters indicators sets this study different (NO_3^-, NO_2^-, NO_2-N, P, PO_4, P_2O_5, NH_4, NH_3, NH_3N, COD, BOD5, dissolved O_2(O2-d), Turbidity (TUR)) and microbiological parameters, namely the input parameter of fecal coliforms, as their existence serves as a significant marker of the influence of human activities on the physicochemical groundwater parameters. The current research seeks to achieve several objectives:

1. Investigate the influences of natural phenomena and human activities on groundwater quality, and determine the sources of groundwater mineralization utilizing multivariate statistical methods and GIS analysis;
2. Assess the magnitude of wastewater influence on the alluvial groundwater within the study area;
3. Determine the physicochemical properties of groundwater to evaluate its suitability for drinking purposes.

MATERIALS AND METHODS

Study area

The region of study is situated in the Merdja plain, which is located at the eastern extremity of Algeria. The following Lambert defines the plain coordinates x = 980,000/1,005,000 E and y = 245,000-258,000 N (Figure 1).

The Merdja plan is a vast area that stretches in a northwest-southeast direction. It is characterized by a relatively flat topography and is surrounded by several mountain ranges. The highlands in the region consist of mountains that reach their highest point at an elevation of 1,470 m. The altitude within the plain ranges from 750 m to 900 m.

The Dyr mountain marks the northern boundary of the Merdja plain, while in the south, it is bordered by the Bouroumane, Doukkane, and Ozmour mountains. The Matlougue mountain defines the western boundary, and the Djebissa mountain forms the eastern boundary.

The Merdja plain itself corresponds to a slump ditch that is filled with continental Plio-Quaternary formations (Fehdi et al., 2016). These formations are supported by the underlying Dano-Montian Marl formation.

Hydrographic network

The digital elevation model (DEM) was used for watershed delineation, extraction of stream networks, and characterization of watershed topography (elevation map, slope map, and aspect map) by using watershed tools in GIS software (Ni et al., 2010). The Shuttle Radar Topographic Mission (SRTM) DEM data that having a resolution of 30m for the study area was downloaded from (EarthExplorer, 2023) Web site.

There are three different relief zones in the study area: the plain, hill and mountain. Using the ArcGIS kernel density function to generate drainage density map, which represents the length of rivers per unit area. The maximum a drainage density value of 1.11 km/km^2 was observed in the Bekkaria zone, along the Wadi El Kebir River, in the Tebessa plain, and in the extreme northeastern part of the study area at the Wadi Chabro exitory. Greater concentrations of streams and rivers are found in locations with high drainage density values, which also suggest relatively high hydrographic network densities. (Moussi & Rebai, 2021).

In the study area, all surface runoff waters from the plain's northern, southern, and eastern regions are collected by the Wadi El Kebir and Chabro Rivers, which then drain the water into the Wadi

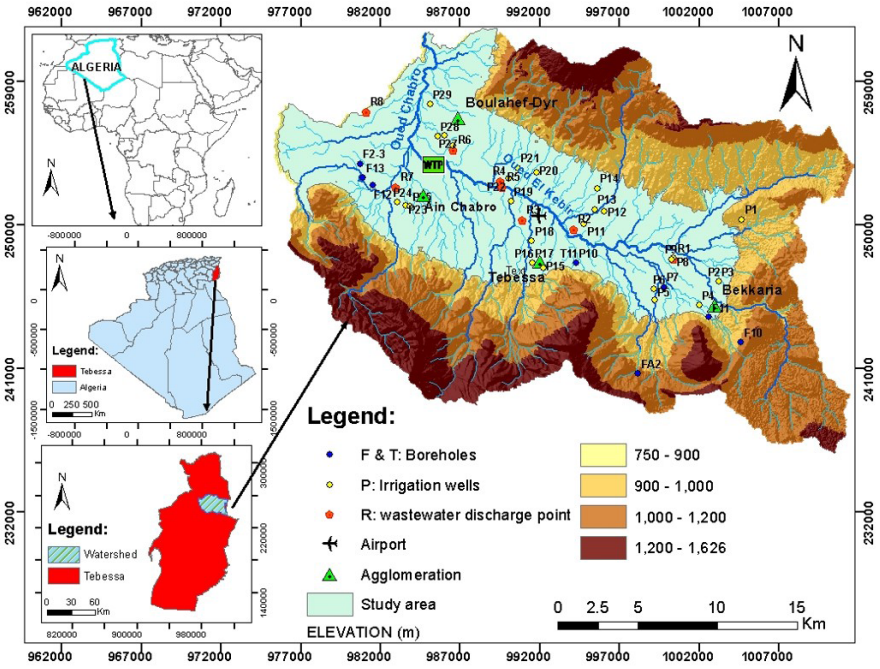

Figure 1. Geographical location of the study area, localization of wastewater discharge points and water samples.

Ksob River. It is worth noting that the majority of the streams have temporary flow, depending on factors such as rainfall and seasonality.

Geological and hydrogeological frameworks

The Tebessa's plio-quaternary tectonic depression (Figure 3) separates the northern Dyr highlands from the southern Doukkane and Mestrie highlands. The Mio-Plio-Quaternary detrital sediments gradually fill this depression (Figure 4) (Fehdi et al., 2016). This depression has passed through four stages: the first in Lower Villafranchien (Upper Pliocene), the second in Upper Villafranchien (Lower Pleistocene), the third at the end of Middle Pleistocene, and the fourth one at the end of Upper Pleistocene. (Kowalski et al., 2002). The majority of the research region was made up of cretaceous limestone deposits, which created an organization of anticlines and synclines. Recent alluvial deposits, gravels, conglomerates, sandstones, and other materials are described as the plio-quaternary and quaternary formations in the central region. The stratigraphic column analysis identified three aquifer formations. The shallow aquifer under study is bounded to the east and west by two large faults that are oriented NW-SE, and it covers the majority of the Tebessa tectonic depression covered by the plio-quaternary formation. The Mio-Pliocene alluvium is composed of gravels encased in an argillaceous matrix that surpasses 350 m in specific locations (Seghir, 2014). For the main sources of recharge, the aquifer primarily receives water from deeper aquifer specifically the Cretaceous formation, through faults.(Drias et al., 2022; Rouabhia et al., 2009); The aquifer's general recharge is influenced by rainfall and other minor sources, such as surface water bodies or localised groundwater flow from adjacent places. Additionally, human activities, such as irrigation or groundwater pumping, can also influence the recharge dynamics of the aquifer.

METHODOOGY

The monitoring of physico-chemical and bacteriological parameters, multivariate statistical techniques like principal component analysis (PCA) and cluster analysis (CA), and the establishment of a spatial variation of the physico-chemical parameters using GIS-based data are the methodologies used in the current study.

Water sampling collection

36 Samples were collected in Feb 2022 in a one-litre polyethylene bottle. The bottles are well rinsed 2-3 times by the sampled water before filling; a sampler from the Tebessa University laboratory was used for collecting samples from the observation wells or when the irrigation pump wasn't operating. The piezometric level was measured only in the static case, The samples were collected directly from the well after 10 min of pumping the well. The samples were stored in a field refrigerator to preserve their natural conditions until they could be sent to the laboratory for analysis. The field refrigerator was used to prevent biological and chemical degradation. (Saha et al., 2019). The samples were filtered using a 0.45 mm cellulose acetate filter. The geographical coordinates of the wells, boreholes, and discharge points were obtained with the help of a handfield GPS device (Garmin). The samples were submitted to physicochemical analyses according to the protocols described by (Rodier et al., 2009) (Table 1). In December 2022, 10 samples were taken from the irrigation wells located near the discharge points and dumping sites (Table 2) for the pollution characterization elements and bacteriological analysis and covering the whole of the study area from the SW to the NE axis following the path of Wadi El Kebir River (P9, P7, P10, P11, P12, P20, P22, P23, P26, and P29 at the extreme NE) (Table 3 and Table 4). A map of the sampling

Table 1. Physico-chemical analysis results (February 2022).

Wells	X	Y	CE	pH	T	HCO_3^-	Cl^-	K^+	Ca^{2+}	Na^+	SO_4^{2-}	TH	Mg^{2+}	TDS	Ionic balance
	(m)	(m)	(µS/cm)		°C	(mg/l)	(mg/l)	(mg/l)	(mg/l)	(mg/l)	(mg/l)	(mg/l)	(mg/l)	(mg/l)	
P1	1004717	250337	7910	6.93	17.5	336	1451	9.7	263.3	876.4	1179.2	584.3	321.0	5062.4	5%
P2	1003245	246427	3260	7.06	18.4	414.8	375.4	9.7	151.8	372.8	469.2	191.8	40.0	2086.4	0%
P3	1003247	246430	8470	6.95	17.4	262.3	1478.1	12.4	243.1	941.0	1026.4	484.1	241.0	5420.8	4%
P4	1002019	244956	1094	6.91	19.1	488	75.7	3.5	77.2	44.3	59.3	144.2	67.0	700.16	0%
P5	999231	245276	1205	7.33	13.5	353.8	193	4.2	92.8	80.0	89.9	143.0	50.2	771.2	-3%
P6	999193	245959	3070	7.22	14.2	414.8	124.9	5.0	211.0	121.0	618.4	304.0	93.0	1964.8	1%
P7	999804	246093	1094	7.51	14	463.6	87.2	6.7	30.3	72.8	28.8	111.3	81.0	700.16	4%
P8	1000417	247936	1011	7.07	20.3	414.8	74.2	4.5	43.1	62.1	44.9	96.2	53.1	647.04	-3%
P9	1000294	247836	1450	6.9	19.9	414.8	120	4.9	81.2	101.0	109.7	142.5	61.3	928	4%
P10	994309	247614	1571	6.79	18	512.4	165	4.0	109.2	87.1	118.6	196.3	87.1	1005.44	3%
P11	994773	250056	6770	7.25	16.5	463.6	1092.7	8.1	243.1	647.3	670.5	443.5	200.4	4332.8	4%
P12	996073	250838	8680	7.04	16.4	439.2	1565.6	9.0	253.3	1019.3	803.5	474.6	221.3	5555.2	5%
P13	995449	250973	8210	6.99	16.7	341.6	1377.6	9.2	269.0	205.0	580.6	566.0	297.0	5254.4	-9%
P14	995633	252298	2760	8.3	15.9	793	337.3	8.9	27.0	426.4	213.9	142.3	115.3	1766.4	5%
P15	992250	247283	2082	6.52	18.5	500.2	177.9	48.9	97.3	102.3	170.8	184.5	87.2	1332.48	3%
P16	991533	247604	2165	6.7	17.5	451.4	224.5	14.6	102.7	116.4	179.8	202.1	99.4	1385.6	3%
P17	991533	247604	1378	7.5	17.5	414.8	94	3.6	58.5	68.6	31.0	120.9	62.4	881.92	5%
P18	991515	248973	2165	6.7	19	414.8	219.6	17.4	112.2	122.1	276.8	220.9	108.7	1385.6	4%
P19	990223	251487	1668	7	18.7	530.7	438.5	1.7	160.9	137.1	242.7	305.8	144.9	1067.52	0%
P20	991800	253281	933	7.17	17.5	414.8	77.2	3.7	60.1	63.6	53.9	111.7	51.6	597.12	0%
P21	990641	253562	1071	6.78	14.7	384.3	77	3.2	55.8	63.6	43.1	106.7	50.9	685.44	2%
P22	990060	252925	1789	7.08	17.5	390.4	258.3	3.6	68.6	132.1	59.3	144.5	75.9	1144.96	2%
P23	983611	251234	4160	6.46	17.8	381.25	670.8	7.2	213.4	272.8	413.4	390.8	177.4	2662.4	5%
P24	983071	251428	1904	6.81	17.5	237.9	194.5	4.7	89.2	87.8	165.4	152.6	63.4	1218.56	3%
P25	983873	251159	2220	6.92	19	317.2	217.5	5.8	109.8	112.0	231.9	201.1	91.3	1420.8	5%
P26	986563	255000	1732	6.75	18.8	375	201.6	3.2	88.2	89.3	95.3	150.3	62.1	1108.48	-1%
P27	986047	255607	1446	6.62	18.5	366	170	3.3	80.9	82.1	80.9	137.8	56.9	925.44	0%
P28	985594	255548	5550	6.46	18.7	475.8	605.4	2.5	218.4	307.8	853.9	433.8	215.4	3552	-1%
P29	985149	257560	5570	6.53	17.5	378.2	890.4	4.3	277.1	337.1	661.50	496.5	219.4	3564.8	2%
F11	1002639	244230	809	6.78	11.5	341.6	39.8	3.4	59.6	35.3	37.70	93.6	34	518	-1%
F12	981537	252466	701	6.94	18	297.07	49.6	2.6	44.4	30.7	25.20	78.1	33.7	449	-3%
F10	1004657	242619	933	7.46	14.6	350	200.2	4.5	70.1	69.3	39.50	131.7	61.6	597	-2%
F09	999804	246093	1439	7.16	18.4	561.2	85.9	3.2	25.4	162.1	140.20	109.3	83.9	921	3%
T11	994309	247614	3100	7.43	13.2	610	63.7	6.6	91.6	230	393.70	174.7	83.1	1984	4%
F2-3	980752	253825	1537	7.11	18.5	281.21	156.7	3.6	72.9	58.6	53.90	120.9	48	984	0%
F13	980919	252941	754	6.96	17.6	270.23	67.8	2.8	50.1	37.1	16.20	85.2	35.1	483	3%

Table 2. Lokalization of wastewater discharges.

Wastewater discharge area	X (m)	Y (m)	Symbol
Bekkaria	1000450.13	247847.909	R1
Wadi Zaarour River	994193.164	249680.694	R2
Wadi Rafana River	990942.329	250274.069	R3
Elatex <upstreame>	989581.949	252719.59	R4
Elatex <downstreame>	989709.657	252328.618	R5
The University	986641.986	254664.666	R6
Ain Chabro	983040.142	252353.44	R7
Wastewater discharge points outlet	981150.426	257060.01	R8

Table 3. Pollution characterization elements analysis (December 2022).

Wells	NO_3 (mg/l)	NO_2 (mg/l)	NO_2N (mg/l)	NH_4 (mg/l)	NH_3 (mg/l)	NH_3N (mg/l)	PO_4 (mg/l)	P (mg/l)	P_2O_5 (mg/l)
P9	29.1	0.13	0.04	0.23	0.22	0.19	0.80	0.20	0.60
P12	58.0	0.19	0.06	6.02	5.68	4.67	0.4	0.3	0.1
P11	22.9	0.13	0.04	0.15	0.14	0.12	2.3	0.8	1.7
P22	31.5	0.17	0.05	0.1	0.09	0.07	0.4	0.1	0.3
P7	12.9	0.01	0.00	0.19	0.18	0.15	0	0	0
P10	15.5	0.10	0.03	0.18	0.17	0.14	0.6	0.2	0.4
P26	10.4	0.02	0.01	0.08	0.08	0.06	0.3	0.1	0.2
P23	16.9	0.03	0.01	0.14	0.13	0.11	0.3	0.1	0.2
P29	9.7	0.01	0.00	0.11	0.1	0.08	0.5	0.2	0.4
P20	15.1	0.02	0.01	1.79	1.68	1.37	0.8	0.3	0.6

Table 4. Microbiologic analysis results (December 2022).

Wells	DCO (mg/l)	DBO5 (mg/l)	TDS (mg/l)	TUR (NTU)	O_2-d (mg/l)	CFT (ufc/100ml)	E-Coli (ufc/100ml)
P9	1806.00	85.92	670.00	2.91	4.41	0	372
P12	517	98.27	8900	2.11	5	0	170
P11	704	85.4	522	4.55	6.32	0	115
P22	1710	75.8	770	0.15	6.62	2	6
P7	1730	108.93	3504	0.68	7.06	0	160
P10	1135	72.78	671	0.1	6.32	7	155
P26	1027	107.13	870	0.14	7.35	17	9
P23	175	122.71	713	0.06	7.65	15	2
P29	1348	97.43	1109	0.84	6.03	3	28
P20	546	88.4	503	1.74	6.32	8	1

points was performed (Figure 1). The in-situ measurement of physicochemical parameters, including electrical conductivity (EC), pH, and temperature, using a Multimeter brand Hach HQ40d coupled to an electrode that is kept in a solution of potassium chloride (KCl) with a concentration of 3 mol/l. The device was previously calibrated by a standard solution and as per user manual calibration steps and tested in the field. The bicarbonate was measured by the titration method, with HCl serving as the standard solution. The chemical parameters were measured at the laboratory of the geology of the Sahara LGS at the University of Ouargla; these analyses are carried out according to four methods:

i. The gravimetric method: for sulfate ions SO_4^{2-} is based on the principle of precipitating sulfates in the form of barium sulfate by the barium chloride as per the chemical reaction: $Ba^{2+} + SO_4^{2-} BaSO_4$.

ii. The flame atomic emission spectrometry method: using a Janeway flame photometer. It is a flame photometer of emission at low temperatures intended for the simultaneous determination of Sodium, Na^+, Potassium K^+, and Calcium Ca^{2+}).

iii. The colorimetric titration method: for the determination of the water hardness TH ($Ca^{2+} + Mg^{2+}$) and bicarbonate (HCO_3^-).

iv. The potentiometric method: used for the determination of chloride ions (Cl^-) using the Titrino 716 apparatus. The chloride is precipitated by silver nitrate in the presence of potassium chromate. The apparatus must be calibrated, and it is allowed to work automatically; at the end, it displays the chloride concentration on its screen.

At the Fethallah laboratory in Tebessa, the pollution chemical parameters indicated measured are the NO_3^-, NO_2^-, NO_2^-N, P, PO_4, P_2O_5, NH_4, NH_3, NH_3N, chemical oxygen demand (COD), biochemical oxygen demand in 5 days (BOD5), dissolved O2 (O2-d) with the Multiparameter and Photometer HANNA HI 83099 COD, and the turbidity (TUR) with the Turbidity meter type HANNA C102 and the bacteriological analysis from the same samples bags and transported to the private laboratory located in the study area and using the field refrigerator in less then six hours from the collection time.

Microbiological analysis method

In order to know the water's bacteriological quality, water sampling campaigns were carried out in December 2022. This allowed us to collect ten water samples from 10 wells around the wastewater dump sites.

Within the framework of this study, only standard germs, indicators of fecal contamination, were examined, and the best represented are fecal coliforms such as *Escherichia Coli* (E-Coli) and total coliforms (TCF). Those samples are taken in sterile plastic bags of 1000 ml with an integrated closure and designated for this type of sampling, leaving air space in the bag to facilitate the suspension of microorganisms by mixing before inoculation in the appropriate culture media, the use of sterile gloves and a gas cylinder while collecting the samples as per as samples collection standards.

The samples were labeled and then stored in a cooler while being transported to the laboratory and analyzed. For these analyses, the membrane filtration (MF) method was applied. For water meant for human consumption, the World Health Organisation (WHO) specifies a bacteriological standard of 0 colonies per 100 ml of filtered water.

GIS analysis of physic-chemical parameters

The UTM-Nord_Algerie_Ancienne projection was utilised in the GIS environment to map the spatial distribution of groundwater quality parameter values. One of the most techniques used for interpolation is the inverse distance weighting method (IDW). The value of an unmeasured location can be estimated by measuring the values surrounding the expected location. (Ajaj et al., 2018). It is essentially based on two assumptions: First, the unknown value of a point has a direct influence on the near control point rather than the far point. Second, the degree of effect of a point is proportional to the inverse of the distance between points. (Ajaj et al., 2018; Diongue et al., 2022).

Multivariate statistical methods

The data collected in the field and the laboratory have been analysed using descriptive and multivariate statistical methods coupled with hydrochemical, geostatistical, and graphical approaches. The statistical approach is based on descriptive statistics, principal component analysis (PCA) and cluster analysis (CA). The PCA is used to study the origin of the mineralization phenomena, the description of the links between the variables by two-dimensional statistical techniques (Mfonka et al., 2015), and identify the major sources of anthropogenic effects on the hydrochemical groundwater quality. PCA is applied to the results of physicochemical analyses on a total of 36 samples with 12 parameters (T°C, Electrical Conductivity (EC), pH, TH, TDS, HCO_3^-, Ca^{2+}, Mg^{2+}, K^+, Na^+, SO_4^{2-}, Cl^-). This method was carried out by R studio (using Facto Mine R, Facto extra, and gg biplot packages) and SPSS software. The Ascending Hierarchical Classification (AHC) or Cluster Analysis (CA) was applied to better understand the hydrogeochemical processes that govern the groundwater in the study area. The two statistical multivariate methods are applied to the results of physicochemical and microbiological analyses on a total of 10 samples with 27 parameters (T°C, EC, pH, TH, TDS, HCO_3^-, Ca^{2+}, Mg^{2+}, K^+, Na^+, SO_4^{2-}, Cl^-, NO_3^-, NO_2^-, NO_2^-N, P, PO_4, P_2O_5, NH_4, NH_3, NH_3N, COD, DBO_5, dissolved O_2(O_2-d), Turbidity (TUR), CFT and E-Coli).

Accuracy of analytical results

Testing the ion balance while accounting for the fact that water is electrically neutral in theory is part of assessing the validity of the results. Consequently, cations total chemical equivalents must be equivalent to anions (Semar et al., 2013). It is important to note that a water chemical analysis is deemed representative only when the ionic balance is 10% or lower. The following Formula 1 determines the calculation of the ionic balance (Akoteyon, 2013):

$$BI = 100*(\Sigma[Cations] - \Sigma[Anions])/(\Sigma[Cations] + \Sigma[Anions]) \quad (1)$$

where Σ [Cations] is the sum of the cations and Σ [Anions] is the sum of the anions (meq/l), and BI is the ionic balance given as a percentage. For each of the 36 analyzed samples, the ionic balance was computed. It is observed that 80% of the sample have an ionic balance (BI) within the range of -5% to +5%, indicating acceptable quality of the analyses. Additionally, 100% of the boreholes have a BI within the range of -10% to +10%, which is considered high but still falls within an acceptable range. Somme analysis had a BI>20% where not accepted due to the use of chloride treatment (boreholes for drinking purposes).

RESULTS AND DISCUSSION

Piezometry

The Tebessa region has been experiencing a period of drought in recent years (Rouabhia et al., 2009; Fehdi et al., 2016; Drias et al., 2022), which has led to the overexploitation of the water table in agricultural areas. As a result, the piezometric level has dropped, and there has been an increase in the mineralization rate in the alluvial groundwater aquifer. Some wells have even become nearly dry.

To assess the piezometric conditions, a survey was conducted in February 2022, and the data collected from the piezometric

readings were used to create a piezometric map of the aquifer during that period (Figure 5).

The piezometric level in the area ranges from 890 to 760 meters. Analysis of the isopiezes curves depicted in reveals two primary flow directions. The first direction is southeast to northwest, following the course of Wadi El Kebir. The second direction is south to north, originating from El Hammamet and extending to Morsott. In the central area, the isopiezes curves exhibit a consistent spacing, indicating a uniform flow pattern.

Furthermore, in the southeast region, the flow axes diverge, indicating recharge from the Djebissa mountain. The isopiezes curves become tighter, suggesting an increasing slope of the piezometric surface and a relatively strong hydraulic gradient toward the center of the plain.

The recharge of groundwater in this aquifer is influenced by factors such as precipitation, infiltration of irrigation water, the presence of quartz sands and Pliocene limestone in the eastern part, and the presence of Serdies Mountain limestone in the western part (Fehdi et al., 2016; Rouabhia et al., 2009).

Hydrochemistry and statistical analysis

The majority of the wells on the plain are haphazardly placed based on agricultural requirements, and their average depth is only 40 meters. The physical and chemical analysis results of the well samples are shown in Table 1. The thematic maps (Figure 6) for the chemical parameters showed that the concentrations of all major ions were highest near P2, P3, and P4 (in the southeast), P11, P12, P13, and P14 (in the north of Tebessa town), and in the northwest part at the Chabro River outlet. This may be caused by similar hydrogeochemical processes. Evaporation in this area is intense, and the groundwater depth is shallow. Furthermore, the decrease in ions concentrations in the northwest part of the study area may be attributed to the impervious layer of natural clay that can slow down the entry of pollutants into the aquifer and reduce the impact of pollutants diffusion (Chu et al., 2020). Figure 7 shows a medium to excellent correlation between these major elements and EC with nitrate (Na^+, SO_4^{2-}, Cl^-, K^+, Ca^{2+} and EC, r^2 = (0.79, 0.5, 0.64, 0.56, 0.32, 0.61) respectively. This correlation reflects the combined influence of rainfall, soil characteristics, and anthropogenic activities on the mineralization and degradation processes within the alluvial aquifer. These factors can affect the concentration of major elements and the electrical conductivity of groundwater, including nitrate contamination.

The nitrate map's regional variation (Figure 8) shows that the average values in the Tebessa, Ain Chabro, and Boulhef-Dyr areas range from 9.7 to 15 mg/l. In contrast, P12 has high levels of 58 mg/l, which are over the WHO's recommended limit of 50 mg/l for drinking water. This well is placed in the crops class, according to the study area's land use map (Figure 2). As a result, the use of nitrate fertilizers is the cause of this high value. The Bekkaria area (well P9) has significant levels of Escherichia coli (372 CFU/100ml) according to the map of geographic variation of the bacteria (Figure 8). This is due to septic tanks, untreated wastewater discharges, animal dung leaching, and domestic animals. Although the concentration range of 2-28 CFU/100ml for this particular germ is low in the Ain Chabro and Boulhef-Dyr locations, it should be highlighted that the presence of any of these types of bacteria makes the water unfit to drink. In consequence, *Escherichia coli* survives only in the digestive systems of humans and warm-blooded animals. As a result, there would be a good correlation between its concentration and the faecal pollution origin. (Zerhouni et al., 2019).

PIPER and DUROV diagrams

Building a Piper trilinear diagram and a Durov plot can help us understand the geochemical evolution of groundwater. Grapher software version 16.2.354 was utilized in the current investigation to create these diagrams. The Piper diagram is a multidimensional plot in which the principal cations (Ca^{2+}, Mg^{2+}, Na^+, and K^+) and anions (HCO_3^-, SO_4^{2-}, and Cl^-) are represented in milliequivalents percentage concentrations in two triangle fields, and then projected farther into the middle diamond field. The Durov diagram is a composite plot made up of two ternary diagrams: a binary plot showing the concentrations of total cations and total anion (meq/l); it defines the hydrochemical processes at effect as well as the types of water that may have an impact on the water genesis. (Ravikumar et al., 2015; Singh & Kumar, 2015).

Data plotted on the Durov diagram (Figure 9) supported three types of hydrochemical processes in the study area. According to Lloyd & Heathcote (1985) classification, Along the dissolving or mixing line, field 5 of the Durov plot contains 60.52% of the sample plot. Weak recent recharge from precipitation or irrigation water infiltration is the cause of this development. Furthermore, a small percentage of samples (21.05%) with Cl^- and Na^+ as the predominant anion / cation highlighted a relationship between ion exchange and rock weathering and groundwater mineralization. Reverse ion exchange has been linked to groundwater, as determined by 18.43% of samples. The Piper trilinear diagram (Figure 10) shows that the majority of the samples (81.57%) belong to the Ca^{2+}-HCO_3^-, mixed Ca^{2+}-Mg^{2+}-Cl^-, and Na^+-Cl^-groups (fields 1, 3 and 2), indicating the dominance of strong acidic anions over weak acidic anions and alkaline earth over alkali (i.e., $Ca^{2+}+Mg^{2+} > Na^+ + K^+$). Rainfall recharge activities from the carbonates border to the north, south, and southeast (Figure 5) are what generate the Ca^{2+}-HCO_3^- water type, which corresponds to low EC values. The groundwater in the research region may contain calcium ions due to the dissolution of $CaCO_3$ and Ca Mg $(CO_3)_2$ precipitates during recharge. This means that ground water in the area is mainly made up of mixtures of earth alkaline metals and has temporary hardness. Most of the water samples are coming in un-polluted to slightly polluted category (Singh & Kumar, 2015). This kind of water facies represents samples comes from boreholes that used for drinking water supply.

Physico-chemical statistical analysis

Descriptive analyses

The descriptive analyses of the physico-chemical elements (Table 5) show that the pH of the analyzed waters varied from 6.46 to 8.3, with a mean of 7 and a standard deviation of 0.36.

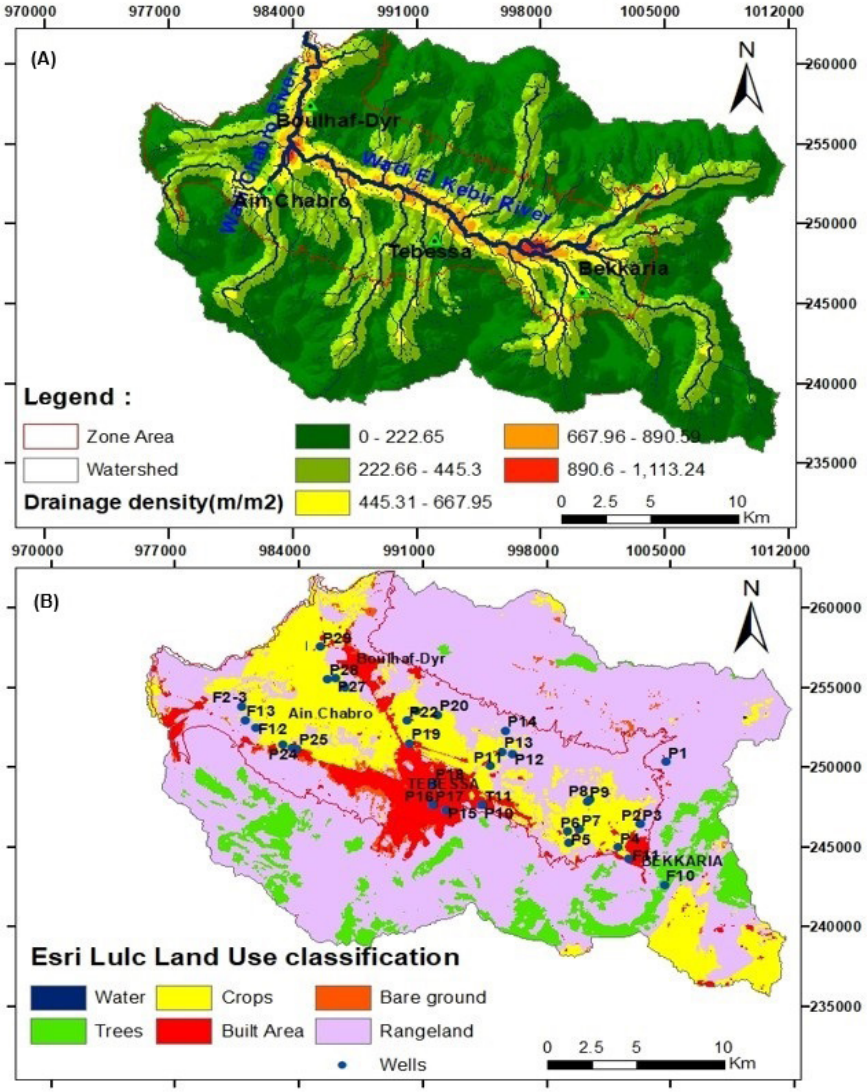

Figure 2. (A) Hydrographic network and drainage density; (B) Land Use in the study area (2022).

Table 5. Descrptive satistics for the water quality parameters in the alluvial aquifer groundwater.

	Total samples	Minimum	Maximum	Mean	standard deviation	Cv	WHO standard
CE (µS/cm)	36	701.00	8680.00	2823.92	2425.63	0.86	400-1500
pH	36	6.46	8.30	7.00	0.36	0.05	6.5-9.5
T C°	36	7.20	20.30	17.2	2.01	0.12	25
HCO-3(mg/l)	36	237.90	793.00	412.69	106.63	0.26	300
Cl- (mg/l)	36	39.80	1565.60	380.52	455.04	1.20	250
K+ (mg/l)	36	1.70	48.90	7.06	8.01	1.13	12
Ca2+ (mg/l)	36	25.40	277.10	119.52	79.10	0.66	75
Na+ (mg/l)	36	30.70	1019.30	215.95	258.68	1.20	200
SO42- (mg/l)	36	16.20	1179.20	285.53	314.07	1.10	200
TH (mg/l)	36	78.10	584.30	227.16	150.95	0.66	50
Mg2+ (mg/l)	36	33.70	321.00	107.64	76.88	0.71	30
TDS (mg/l)	36	448.64	5555.20	1790.89	1568.61	0.86	1000

The pH values are relatively acidic to neutral. The temperature of the waters varies between 11.5 and 20.3 °C, with an average of 17.27 °C and a standard deviation of 2.01 °C. The electrical conductivities of these waters varied from 701 to 8680 µS/cm, with an average of 2724 µS.cm/l and a standard deviation of 2425 µS/cm; 69% of the values are outside the WHO potability

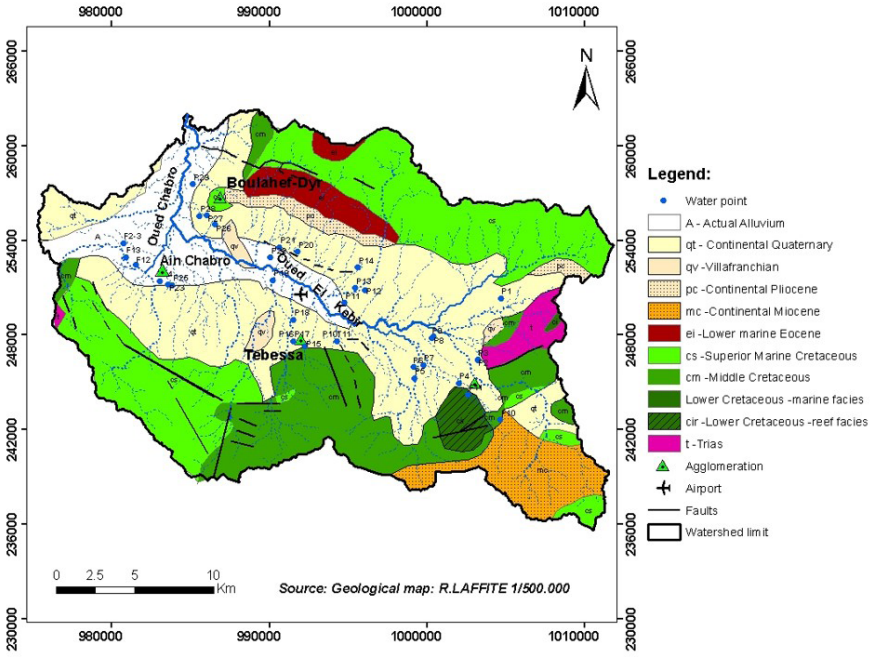

Figure 3. Geological map of the study area.

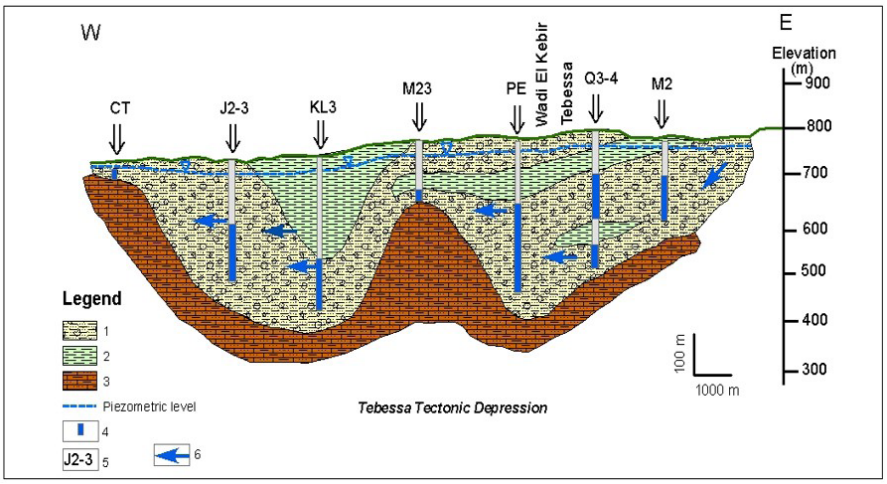

Figure 4. Hydrogeological cross-section through the Tebessa plain. Modified from Rouabhia et al. (2009) and Drias et al. (2022).
(1) Permeable zone (marly-limestones, alluvial fans, silts, calcareous crust, conglomerates, and gravels); (2) Impermeable zone (clay and marl); (3) Marly bedrock; (4) Screened interval; (5) Well name. Elevations are above sea level; (6) Water flow direction.

standard (400-1500 µS/cm). For major cations (Ca^{2+}, Mg^{2+}, Na^{+}, and K^{+}), Na^{+} ions are the most predominant and vary between 30.7 and 1019.3 mg/l, with an average of 216 mg/l and a standard deviation of 258.7 mg/l. Next comes the Mg^{2+} ions with a variation of 33.7 to 321 mg/l, an average of 107.6 mg/l, and a standard deviation of 76.9 mg/l. Ca^{2+} ions occupy the third position and varied between 25.4 and 277.1 mg/l, with a mean of 119.5 mg/l and a standard deviation of 79.1 mg/l. K+ ions occupy the last position and vary from 1.7 to 48.9 mg/l, with a mean of 7.06 mg/l and a standard deviation of 8.01 mg/l. Concerning the major anions (HCO_3^-, Cl^-, SO_4^{2-}), Cl^- ions predominate and varied from 39.8 to 1565.6 mg/l, with a mean of 380.52 mg/l and a standard deviation of 455 mg/l. Next comes SO_4^{2-} ions with a variation of 16.2 to 1179.2 mg/l, a mean of 285.53 mg/l and a standard deviation of 314 mg/l. HCO_3^- ions occupy the third position and vary from 237.9 to 793 mg/l, with a mean of 412.7 mg/l and a standard deviation of 106.63 mg/l.

Principal omponent analysis (PCA) for the physico-chemical parameters

Principal component analysis was performed on 36 samples and 12 parameters (pH, T°, EC, SO_4^{2-}, K^{+}, Na^{+}, Ca^{2+}, Mg^{2+}, TH,

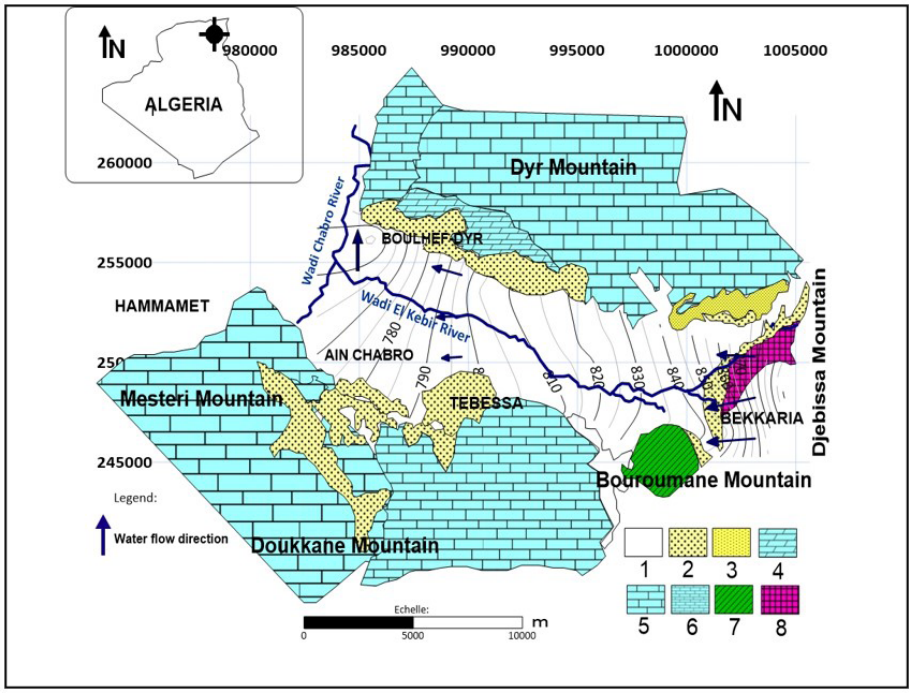

Figure 5. Geologic and piezometric map of study area (February 2022).
(1) Recent alluvium; (2) Conglomerate and gravel; (3) Sand; (4) Turonian limestone; (5) Maastrichtian limestone; (6) Eocene limestone; (7) Cenomanian marl; (8) Triassic formations.

Table 6. Correlation matrix of physico-chemical parameters.

	CE	pH	T	HCO^-_3	Cl^-	K^+	Ca^{2+}	Na^+	SO_4^{2-}	TH	Mg^{2+}	TDS
	µS/cm		°C	mg/l	mg/l	mg/l	mg/l	mg/l	mg/l	mg/l	mg/l	mg/l
CE (µS/cm)	**1.000**											
pH	-0.123	**1.000**										
T (°C)	0.011	-0.394	**1.000**									
HCO^-_3 (mg/l)	-0.051	**0.457**	-0.074	**1.000**								
Cl^- (mg/l)	**0.960**	-0.111	0.033	-0.136	**1.000**							
K^+ (mg/l)	0.166	-0.197	0.109	0.158	0.128	**1.000**						
Ca^{2+} (mg/l)	**0.894**	-0.327	0.037	-0.163	0.866	0.113	**1.000**					
Na^+ (mg/l)	**0.871**	0.072	-0.021	0.050	0.880	0.146	**0.697**	**1.000**				
SO_4^{2-} (mg/l)	**0.927**	-0.154	-0.002	-0.038	0.862	0.140	**0.897**	**0.853**	**1.000**			
TH (mg/l)	**0.939**	-0.252	0.051	-0.081	0.924	0.132	**0.969**	**0.750**	**0.917**	**1.000**		
Mg^{2+} (mg/l)	**0.923**	-0.159	0.061	0.008	0.923	0.143	**0.873**	**0.755**	**0.877**	**0.967**	**1.000**	
TDS (mg/l)	**1.000**	-0.123	0.011	-0.051	0.960	0.166	**0.894**	**0.871**	**0.927**	**0.939**	**0.923**	**1.000**

HCO_3^-, Cl^- TDS). This analysis allows us to calculate the eigenvalues, the variances expressed for each factorial axis, their accumulation, the correlation coefficients between all the parameters taken two by two, the descriptive statistics, and the participation of each parameter on the plan of the factorial axes. The different correlations observed between various elements in the correlation matrix (Table 6) indicate

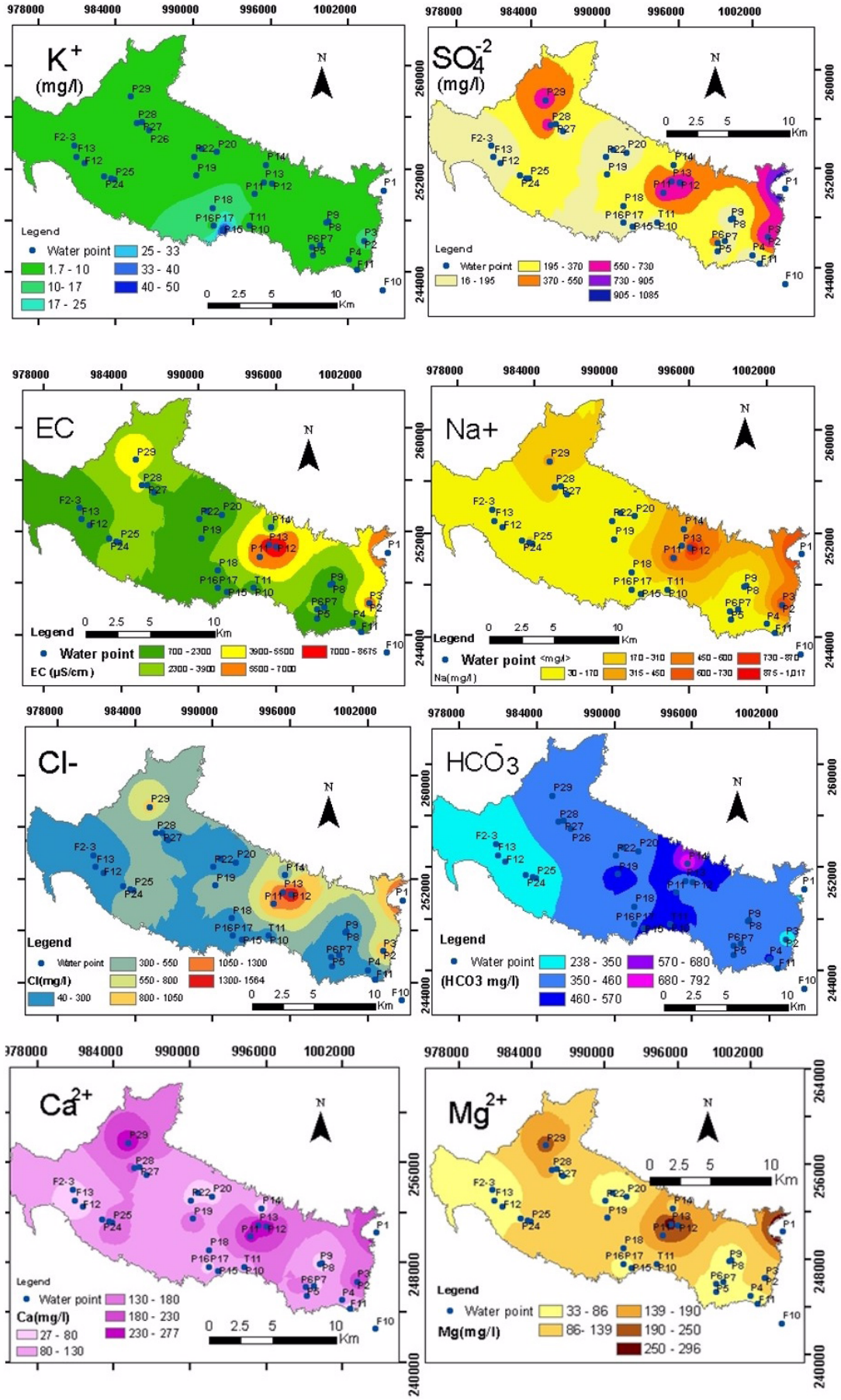

Figure 6. Thematic maps for the physico-chemical parameters of the alluvial aquifer.

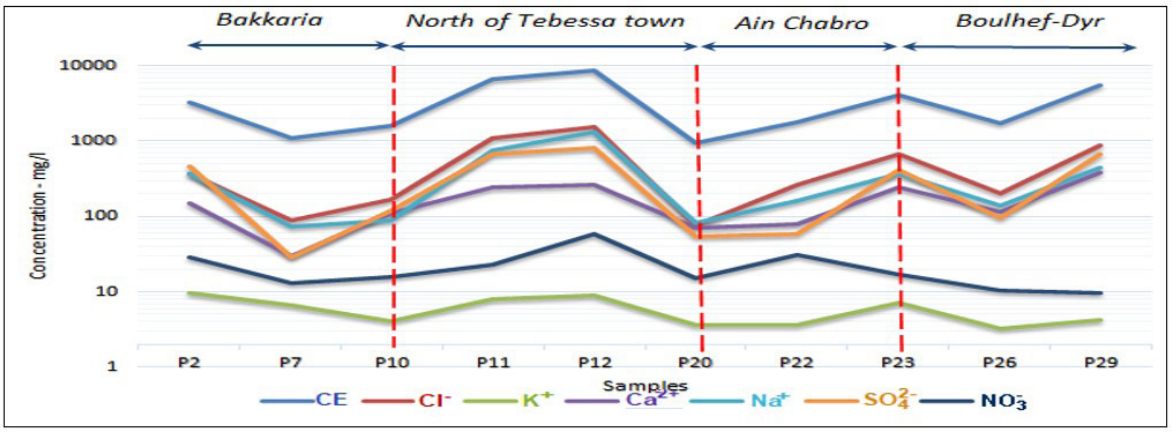

Figure 7. Correlation between major elements EC, Cl-, K+, Ca2+, Na+, SO42- with NO3- from SW-NE.

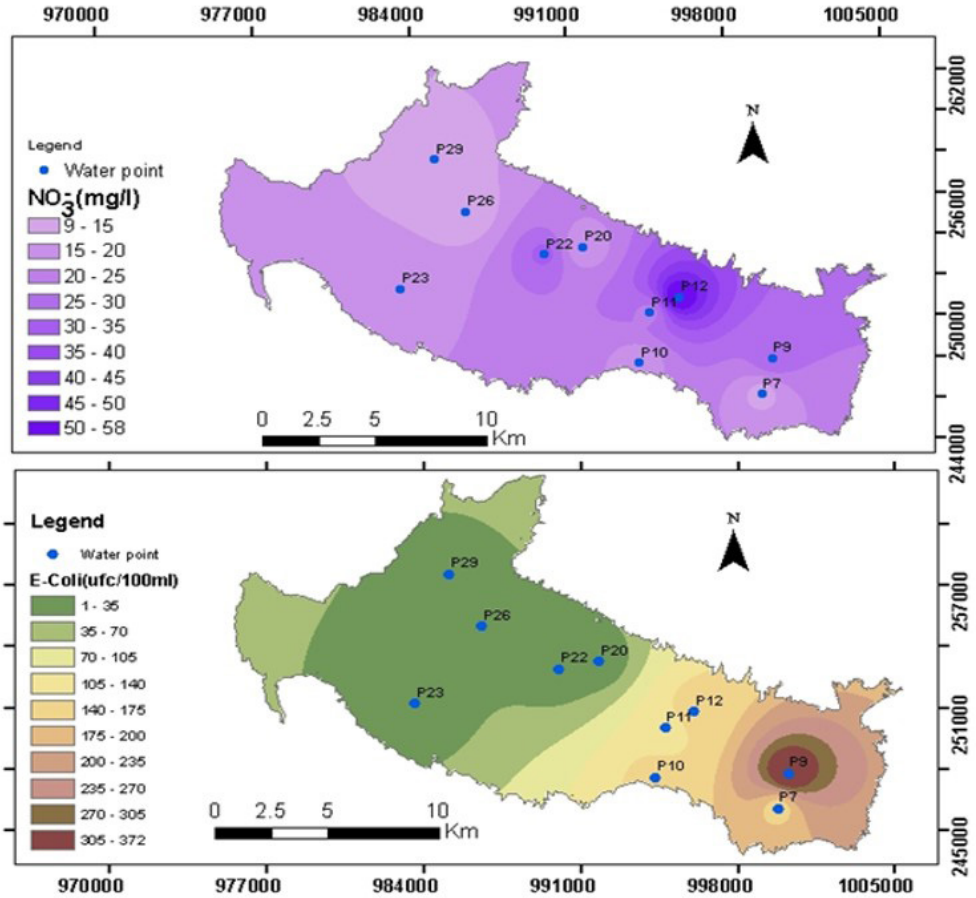

Figure 8. Spatial distribution of NO3- and E-Coli concentration in the study area.

their origin (Djahadi et al., 2022). SO_4^{2-}, Na^+, Ca^{2+}, Mg^{2+}, and Cl^- ions control the mineralization of the waters in the area. The strong correlations between SO_4^{2-} with Na^+(0.85), Ca^{2+}(0.9), Mg^{2+}(0.88), and Cl^-(0.86) ions, as well as their clustering around the main axis of mineralization F1 (Figure 11), indicate that they probably come from the same mechanism and origin (residence time in the aquifer and soil rainfall). Temperature is the only physical parameter that is almost not correlated with any parameter; the pH has a mean correlation with representing HCO_3^- ions (0.46). The coefficient of variation 'Cv' will give a general view of the hydrochemical alluvial groundwater homogeneity by its value, it is the standard deviation ratio to the mean, and the (Cv) is more than 0.25 in all parameters except pH and temperature, which shows heterogeneity of the alluvial groundwater (Moussa et al., 2018). The three primary principal components that are the primary determinants of groundwater in this area were extracted using the Varimax approach with Kaiser

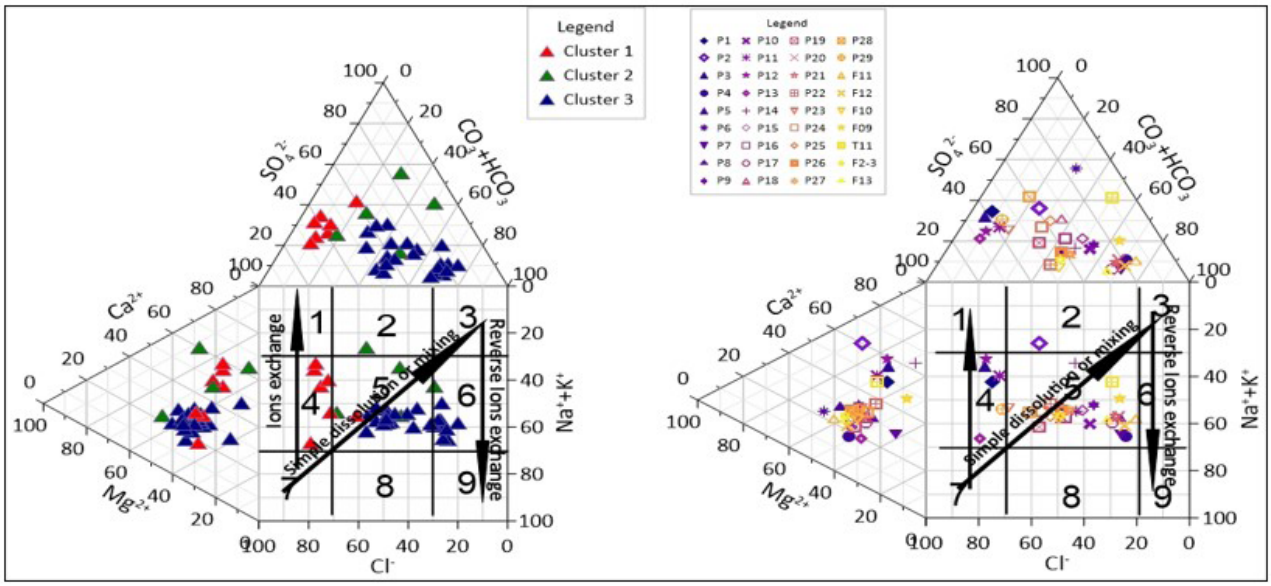

Figure 9. Clusters & groundwater samples analysis and their plots on Durov's diagram.

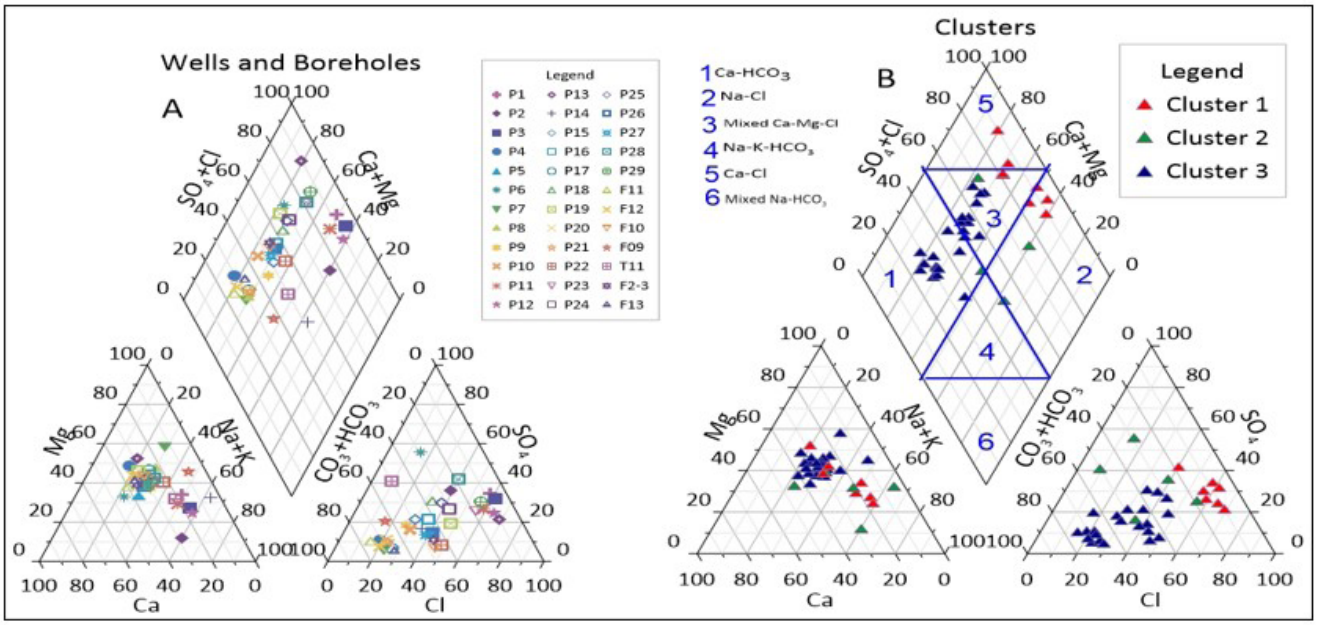

Figure 10. Piper Trilinear diagram classifying major hydrochemical facies. (A) Samples facies; (B) Clusters facies.

normalization, which was used for the rotation of the principal components. Table 7 shows that the first three axes express 84.96% of the total variance, F1 alone expresses more than 61.15% of the information. The PCA of a region is only valid if the percentage of total cumulative variance is greater than 70% (Soro et al., 2019), 14.1% for the second, and 9.7% for the third. The first three axes are given sufficient total variance to provide information on the different hydrogeochemical parameters of the aquifer.

Figure 11 shows the distribution of physico-chemical parameters on the F1-F2 factorial plane. A high positive correlation of CE, Cl^-, SO_4^{2-}, Na^+, TH, Ca^{2+}, Mg^{2+}, and TDS constitutes the F1 factor, accounting for 66.6% of all parameters examined. Consequently, this component clarifies the overall water quality characteristics that are crucial for drinking water. The grouping of these elements suggests the origin of a common source and an identical mechanism of the solution of these elements; as a result of human activity, the ratios of Na^+, Cl^-, and SO_4^{2-} are increasing. The F1 axis controls the major process of mineralization by the residence time in the aquifer and soil rainfall. Table 8 shows the correlation of these parameters with its factorial axes. Factor F2 represented 14.1% of the variance and had an excellent correlation by the temperature (0.711), reverse correlation with pH.

The third factorial axis F3, represents 9.7% of the total variance; it's high and positively correlated with potassium (0.71)

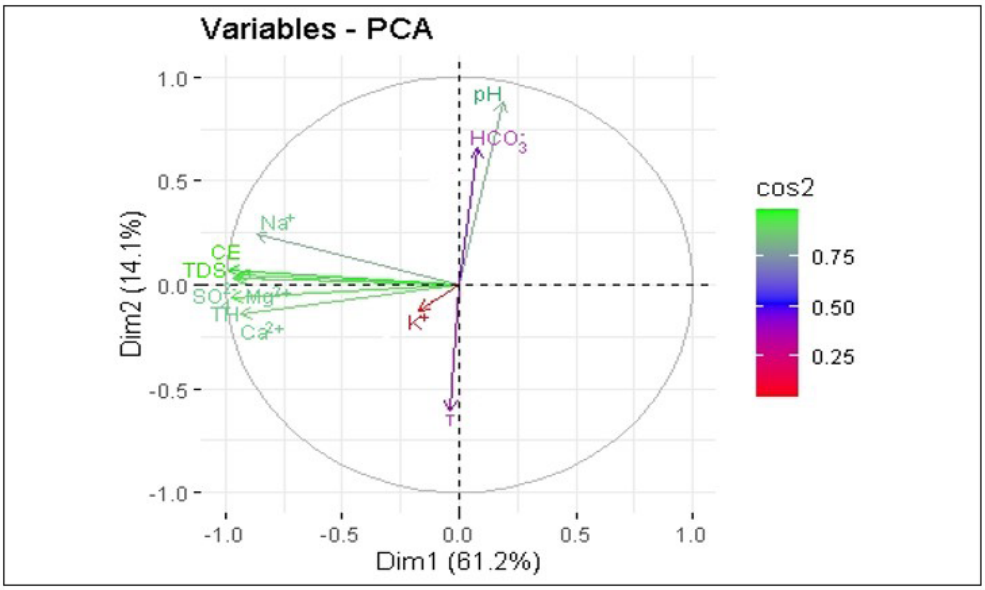

Figure 11. Correlation cercle for the physico-chemical parameters in the plan F1-F2.

Table 7. Eigen values and percentages expressed for the three main factorial axes of physico-chemical parameters analyses.

Component	Initial Eigen values			Rotation Sums of Squared Loadings		
	Total	% of variance	Cumulative %	Total	% of variance	Cumulative %
1	7.331	61.092	61.092	7.331	61.157	61.157
2	1.689	14.072	75.164	1.689	14.093	75.25
3	1.165	9.707	84.871	1.165	9.707	**84.96**
4	0.799	6.655	91.526			
5	0.489	4.079	95.605			
6	0.236	1.968	97.572			
7	0.144	1.203	98.776			
8	0.077	0.646	99.421			
9	0.065	0.539	99.960			
10	0.005	0.040	100.000			
11	1.153E-15	9.609E-15	100.000			
12	1.965E-16	1.638E-15	100.000			

Table 8. Correlation of the physico-chemical parameters with their factorial axes.

Parameters	Components		
	1	2	3
EC (µS/cm)	**0.986**	0.029	0.037
pH	-0.119	-0.859	0.257
T C°	-0.025	**0.711**	0.151
HCO^-_3(mg/l)	-0.056	-0.409	**0.777**
Cl^- (mg/l)	**0.968**	0.035	-0.031
K^+ (mg/l)	0.126	0.423	**0.710**
Ca^{2+} (mg/l)	**0.925**	0.183	-0.113
Na^+ (mg/l)	**0.880**	-0.133	0.136
SO_4^{2-} (mg/l)	**0.952**	0.034	0.021
TH (mg/l)	**0.967**	0.132	-0.030
Mg^{2+} (mg/l)	**0.947**	0.071	0.057
TDS (mg/l)	**0.986**	0.029	0.037

and bicarbonate (0.78). The F3 is thought to be an axis that represents the pollution in agriculture brought on by fertilisers use. As a result, the F1 axis represents salinity, while the second axis represents temperature. At the same time, we discovered that axis F3 represents the alkalinity axis.

Cluser Analysis (CA)

A data analysis tool called cluster analysis is used to organize data with similar properties; this tool is a multivariable statistical technique applied to analyze the correlation between the physicochemical parameters and group them into clusters. In this study, a dendrogram is constructed to classify each individual's water type (Figure 12). Based on the degree of similarity, the resulting dendrogram proposes three groups. Individuals within the same group are connected by a small distance based on their similarity (Modibo Sidibé et al., 2019). The Ward aggregation criterion and the Euclidean distance between variables were used in the CA multivariate statistical technique using Rstudio software. Twelve variables and thirty-six observations (wells samples and boreholes) were categorised hierarchically and examining the results of the analysis under the dendrogram in Figure 12. There are three distinct groups or classifications were distinguished. The first class includes the closest points P23, P28, P29, P11, P13, P12, P1 and P3. This class is characterised by high contents of physicochemical parameters, especially EC (>3000µS/cm), Na^+, Ca^{2+}, Mg_{2+}, Cl^-, SO_4^{2-}, TH, and TDS. From the PCA results, this class represents the F1 factor that occupied the highest anthropogenic area activities in the northeast part and the north of Tebessa town. On the other hand, the second class includes points P26, P27, P8, P9, F2-3, F12, F13, P24, P25, P21, F11, P17, P20, P7, P5 and F10 which have low EC (700-1500µS/cm). The third one includes the rest points and has a medium mineralization and EC (1500-3000µS/cm).

Space analyses of the individuals

We will examine the organisation of individuals according to their projections on the F1-F2 plane (Figure 13). The physicochemical characteristics divide the study area into three groups. Individuals in the first group correspond to waters with high mineralization, have chloride sodium and potassium facies, and occupy the negative side of the axe; the second group represents individuals that has low mineralization and occupy the positive side of the axe, when the TDS ranged from 450-700 mg/l, and according to the Piper diagram have bicarbonate calcic and magnesian facies; and the third group have a moderately mineralized waters, and presented by chloride and sulphate calcic and magnesian facies. This event typically reflects the variability of samples collected from the basin's upstream and downstream parts. The waters from the carbonate, limestone, and marl aquifers are mostly of low salinity, whereas the waters from the aquifers containing evaporitic rocks in the southwestern part next to Djebissa mountain are more saline (water-rock contact), confirming the hypothesis of contamination of the waters by the phenomenon of dissolution controlled by the lithological variation caused by the change of geological domains.

Physico-chemical and microbiological statistical analysis

Principal component analysis (pca) of total physicochemical and microbiological parameters

This analysis was performed on ten samples collected near the discharge points in order to investigate the vulnerability of groundwater to pollution and to study the origin of mineral

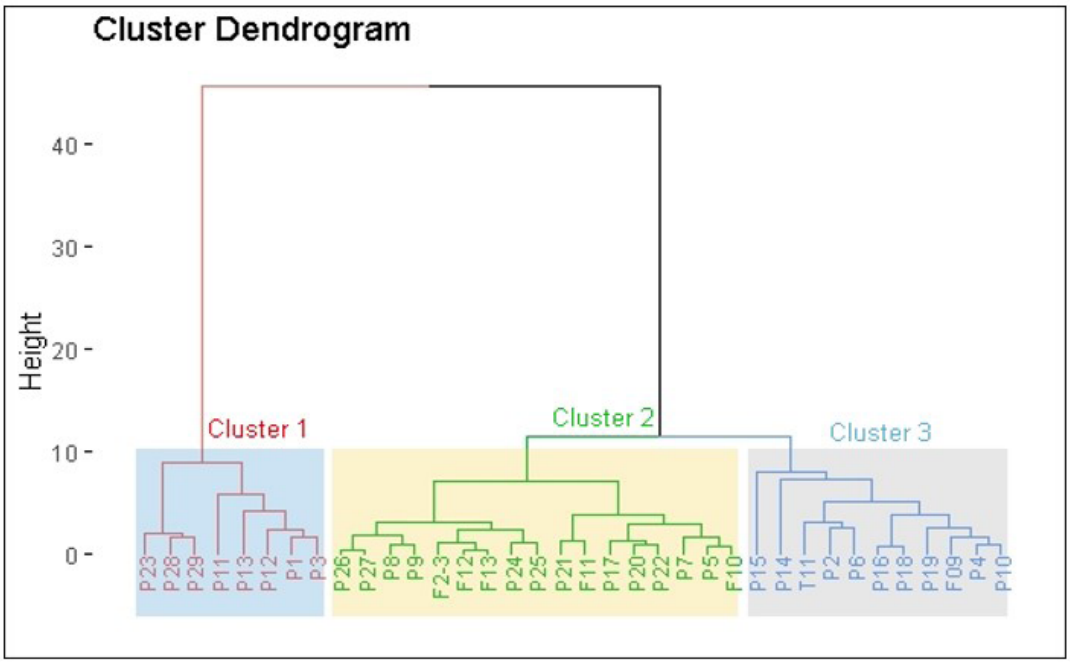

Figure 12. Dendrogram of 36 alluvial groundwater samples points.

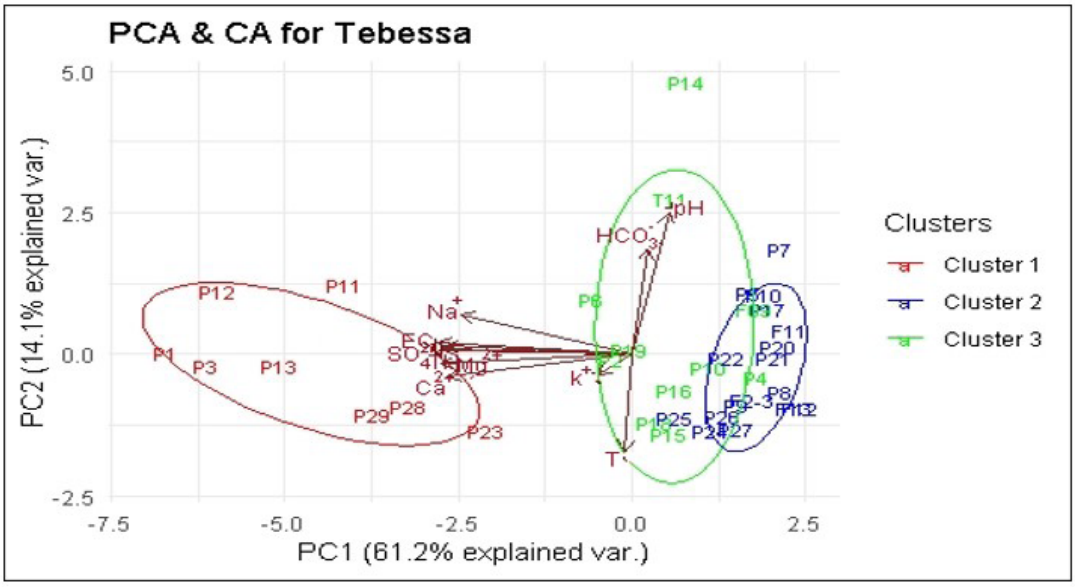

Figure 13. Individuals space analysis in the factorial plan F1-F2.

elements and the geochemical processes that lead to groundwater mineralization. This analysis was applied to 27 parameters (T°C, EC, pH, TH, TDS, HCO_3^-, Ca^{2+}, Mg^{2+}, K^+, Na^+, SO_4^{2-}, Cl^-, NO_3^-, NO_2^-, NO_2-N, P, PO_4, P_2O_5, NH_4, NH_3, NH_3N, COD, BOD5, Dissolved O_2(O2-d), Turbidity (TUR), Total Coliforms CFT and *Escherichia coli* (E.- Coli). Each hydrochemical parameter's degree of contribution to the groundwater mineralization was determined by computing the correlation matrix (Mejri et al., 2018). The bivariate correlation matrix for 27 physicochemical and microbiological elements was presented in (Table 9):

- Temperature and pH are almost not correlated with any parameter;
- The EC shows a moderate correlation with NO_3^-, NH_4, NH_3, NH_3N, Mg^{2+}, Ca^{2+}, excellent correlation with TDS, K^+, Na^+, SO_4^{2-}, Cl^- (r^2 = 0.83 to 0.96). Nitrate NO_3^- shows an excellent correlation with nitrite NO_2^-, nitrite nitrogen NO_2-N, ammonia NH_3, ammonia nitrogen NH_3^- and ammonium NH_4 (r^2 = 0.81 to 0.86). This correlation is due to the ammonium ion being transformed rather quickly into nitrates and nitrites by oxidation. A strong presence of ammoniacal nitrogen is an indication of pollution by discharges of human or industrial origin (chemical industries, nitrogenous fertilizers, textile industries. A nitrite ion is an intermediate form between the ammonium ion and the nitrate ions (Observatory of the Environment in Brittany, 2023)- However, a moderate correlation (r^2=0.5) between the potassium and nitrate measurements indicates their origin (chemical fertilizer dissolution). Furthermore, a substantial correlation between Cl^- and K^+ (0.74) implies that part of the chlorides originate from KCl dissolution (Houria et al., 2020).
- Finally, Cl^- and Na^+ were well correlated with NH_4, NH_3, NH_3-N. The primary lithogenic sources of chloride in groundwater are thought to be the weathering of halite and evaporite and the dissolving of salt deposits, and the anthropogenic sources (Tiwari & Singh, 2014). Anthropogenic sources of chloride are septic, agricultural activity, wastewater discharges, domestic and industrial waste (Fehdi et al., 2009). We observed these maximum values at the towers of the Bekkaria zone. Table 10 shows the distribution of the eigenvalues of the different principal components. A total of four factorial axes or principal components were selected: F1, F2, F3, and F4. The variance expressed by these four components is (84.9%), and it is significant enough to provide information on the different hydrogeochemical parameters of the aquifer. Thus, 42.9% of the dataset's variability was explained by the F1 factor, whereas 19.1%, 14.1%, and 8.85% were explained by the F2, F3, and F4 factors, respectively. The variable loading values are listed in (Table 11). A value near one suggests a strong relationship between the factors and variables. These loads are further categorized as high (>0.75), moderate (between 0.75 and 0.50), and low (between 0.50 and 0.30). F1 exhibited a moderate association with K^+ and a high positive relationship with EC, Cl^-, Mg^{2+}, Ca^{2+}, Na^+, SO_4^{-2}, TH, and TDS (Figure 14). Possible sources of SO_4^{2-} include oxidation of sulfur compounds and fertilizer produced SO_4^{2-}. However, man-made factors, such as the quality of irrigation water. Uncontrolled fertilization is likely the cause of Ca^{2+}, Na^+, and Mg^{2+}. Moreover, the chlorides might have been brought on by the weathering of the soil and the formation of salts. Alkaline water permeated the rocks and soil, as evidenced by the modest link between F2 and NO_2 and the high correlation between F2 and NO_3^-, NO_2N, NH_4, NH_3, and NH_3N. These findings explain the processes by which human behavior occurs characterized by descriptors of rainfall leaching, anthropogenic pollution, and water quality indicators (Akoteyon, 2013; Alamdar et al., 2019). The F3 axis, consisting of a positive correlation with P, PO_4, P_2O_5 and TUR, represents 14.1% of the total

Table 9. Correlation matrix between the different physico-chemical and pollution parameters indicators.

	EC	pH	T	HCO^-_3	Cl^-	K^+	Ca^{2+}	Na^+	SO^{-2}_4	TH	Mg^{+2}	NO_3	NO_2	NO_2N	NH_4	NH_3	NH_3N	PO_4	P	P_2O_5	COD	DBO5	TDS	TUR	O_2d	CFT	E-Coli
EC	**1.00**																										
pH	-0.14	1.00																									
T	-0.29	-0.49	1.00																								
HCO^-_3	0.00	0.49	-0.46	1.00																							
Cl^-	**1.00**	-0.13	-0.29	-0.01	**1.00**																						
K^+	**0.74**	0.25	**-0.60**	0.29	**0.74**	**1.00**																					
Ca^{+2}	**0.92**	-0.45	-0.16	-0.12	**0.90**	**0.55**	1.00																				
Na^+	**0.96**	0.06	-0.32	0.12	**0.97**	**0.79**	0.77	**1.00**																			
SO^{-2}_4	**0.98**	-0.23	-0.28	-0.03	**0.97**	**0.68**	0.97	**0.90**	**1.00**																		
TH	**0.94**	-0.38	-0.24	-0.08	**0.92**	**0.62**	0.99	**0.80**	**0.98**	**1.00**																	
Mg^{2+}	**0.94**	-0.28	-0.34	-0.04	**0.93**	**0.68**	0.97	**0.82**	**0.97**	**0.99**	**1.00**																
NO^-_3	**0.56**	0.20	0.06	0.11	**0.59**	**0.54**	0.27	**0.73**	0.44	0.30	0.33	**1.00**															
NO^-_2	0.39	0.21	0.31	0.27	0.41	0.33	0.17	**0.54**	0.28	0.17	0.18	**0.85**	**1.00**														
NO_2N	0.39	0.20	0.33	0.25	0.41	0.33	0.16	**0.55**	0.27	0.16	0.15	**0.87**	**0.99**	**1.00**													
NH_4	**0.58**	0.17	-0.26	0.12	**0.62**	**0.51**	0.32	**0.74**	**0.49**	0.35	0.37	**0.81**	0.46	**0.50**	**1.00**												
NH_3	**0.58**	0.17	-0.26	0.12	**0.62**	**0.51**	0.32	**0.74**	**0.49**	0.35	0.37	**0.81**	0.46	**0.50**	**1.00**	**1.00**											
NH_3N	**0.58**	0.17	-0.26	0.12	**0.62**	**0.51**	0.32	**0.74**	**0.49**	0.35	0.37	**0.81**	0.46	**0.50**	**1.00**	**1.00**	**1.00**										
PO_4	0.36	0.22	0.00	0.29	0.31	0.27	0.35	0.34	0.37	0.32	0.28	0.05	0.31	0.32	-0.10	-0.11	-0.10	**1.00**									
P	0.55	0.24	-0.14	0.32	0.52	0.42	0.49	**0.55**	**0.55**	0.47	0.44	0.20	0.36	0.38	0.14	0.14	0.14	**0.96**	**1.00**								
P_2O_5	0.27	0.21	0.03	0.25	0.22	0.19	0.29	0.23	0.30	0.26	0.22	-0.06	0.23	0.24	-0.22	-0.22	-0.22	**0.99**	**0.92**	**1.00**							
COD	-0.49	0.27	0.20	0.06	-0.50	-0.43	-0.51	-0.47	-0.48	-0.49	-0.46	-0.13	0.08	0.01	-0.42	-0.42	-0.42	-0.23	-0.37	-0.16	**1.00**						
DBO5	0.17	-0.26	-0.40	-0.44	0.17	0.36	0.21	0.09	0.18	0.24	0.27	-0.19	-0.56	-0.54	0.05	0.05	0.05	-0.41	-0.34	-0.41	-0.38	**1.00**					
TDS	**1.00**	-0.14	-0.29	0.00	**1.00**	**0.74**	**0.92**	**0.96**	**0.98**	**0.94**	**0.94**	**0.56**	0.39	0.39	**0.58**	**0.58**	**0.58**	0.36	0.55	0.27	-0.49	0.17	**1.00**				
TUR	0.44	0.41	-0.15	0.26	0.41	**0.49**	0.31	0.50	0.43	0.30	0.29	0.35	0.40	0.42	0.22	0.22	0.22	**0.84**	**0.85**	**0.80**	-0.11	-0.26	0.44	**1.00**			
O_2d	-0.27	-0.10	-0.19	-0.19	-0.27	-0.16	-0.16	-0.37	-0.27	-0.14	-0.12	-0.61	-0.59	-0.58	**-0.47**	**-0.47**	**-0.47**	-0.23	-0.27	-0.18	-0.25	0.47	-0.27	-0.57	**1.00**		
CFT	-0.28	-0.58	0.26	-0.42	-0.27	-0.37	-0.09	-0.37	-0.26	-0.15	-0.22	-0.48	-0.54	-0.47	-0.25	-0.25	-0.25	-0.30	-0.33	-0.27	-0.47	0.47	-0.28	-0.56	**0.66**	**1.00**	
E-Coli	-0.01	0.24	-0.01	0.46	-0.03	0.27	-0.13	0.10	-0.03	-0.12	-0.11	0.37	0.42	0.40	0.14	0.14	0.14	0.14	0.09	0.11	0.43	-0.26	-0.01	0.48	**-0.75**	-0.57	**1.00**

Table 10. Eigen values and percentages expressed for the three main axes for total physicochemical and microbiological analyses.

Component	Initial eigen values			Sums extracted from the charges square		
	Total	% of variance	cumulative %	Total	% of variance	cumulative %
1	11.576	42.876	42.876	11.576	42.876	42.876
2	5.154	19.087	61.963	5.154	19.087	61.963
3	3.804	14.088	76.051	3.804	14.088	76.051
4	2.391	8.854	84.905	2.391	8.854	**84.905**
5	1.547	5.728	90.634	1.547	5.728	90.634
6	0.919	3.402	94.036			
7	0.769	2.849	96.885			
8	0.719	2.665	99.550			
9	0.122	0.450	100.000			

Table 11. Correlation of total physicochemical and microbiological parameters with their factorial axes.

Parameters	component			
	1	2	3	4
EC	**0.914**	0.345	0.176	0.010
pH	-0.368	0.225	0.294	0.243
T	-0.297	0.054	0.113	0.097
HCO^-_3	-0.146	0.132	0.340	0.294
Cl^-	**0.898**	0.395	0.144	-0.006
K^+	**0.648**	0.321	0.113	0.075
Ca^{2+}	**0.966**	0.057	0.147	-0.075
Na^+	**0.773**	0.563	0.199	0.060
SO_4^{2-}	**0.957**	0.213	0.171	0.008
TH	**0.981**	0.067	0.113	-0.054
Mg^{+2}	**0.981**	0.079	0.066	-0.025
NO^-_3	0.271	**0.870**	0.041	0.345
NO^-_2	0.099	**0.666**	0.357	0.487
NO_2N	0.077	**0.717**	0.381	0.417
NH_4	0.318	**0.891**	-0.129	0.000
NH_3	0.318	**0.891**	-0.130	0.000
NH_3N	0.320	**0.891**	-0.129	0.003
PO_4	0.235	-0.082	**0.962**	0.055
P	0.383	0.100	**0.902**	-0.006
P_2O_5	0.183	-0.192	**0.957**	0.055
COD	-0.416	-0.325	-0.193	**0.753**
DBO_5	0.366	-0.188	-0.555	-0.455
TDS	**0.914**	0.345	0.176	0.010
TUR	0.289	0.149	**0.745**	0.323
O_2-d	-0.138	-0.431	-0.179	-0.732
CFT	-0.158	-0.177	-0.235	-0.805
E-Coli	-0.060	0.136	0.082	**0.807**

variance; the main sources of phosphates in water are industrial effluents, wastewater discharges (which contain synthetic detergents with phosphate bases), and land runoff from farming operations that employed inorganic fertilizers (Lewoyehu, 2021). The factorial plan F4 correlated with E-Coli and COD, this axe represente the hygienic quality of water.

Cluster analyses

In order to complete the interpretation of the PCA, a hierarchical ascending classification was performed. The technique used is a variance aggregation technique or Ward's method based on the calculation of the Euclidean distances between statements. The variance aggregation techniques attempt to optimize, according

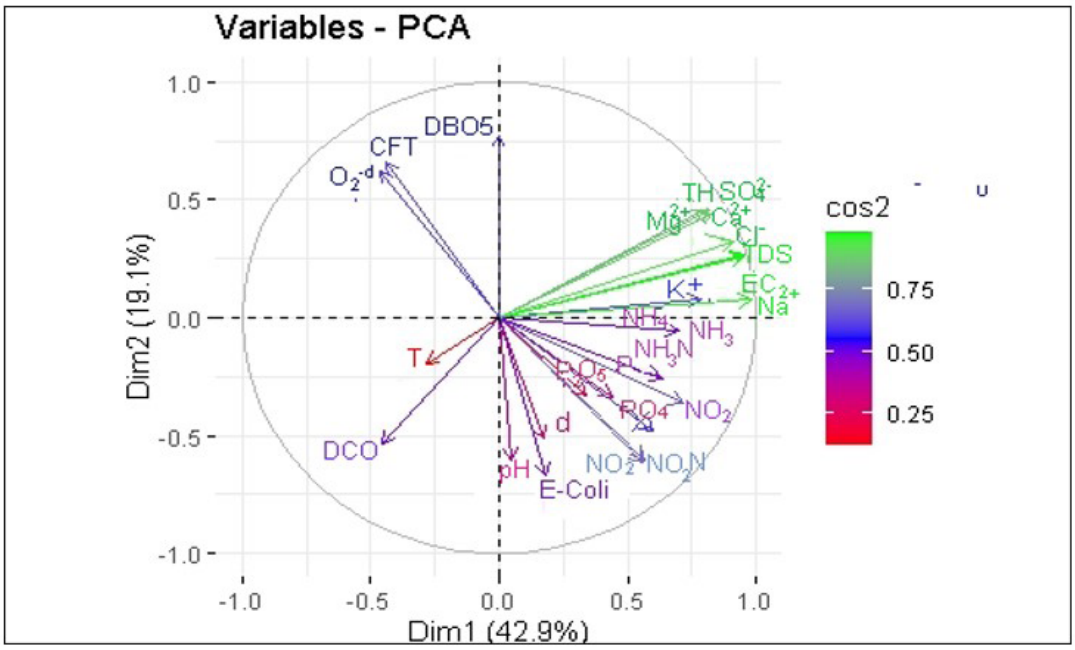

Figure 14. Correlation circle of physico-chemical and microbiological parameters on F1-F2 plane.

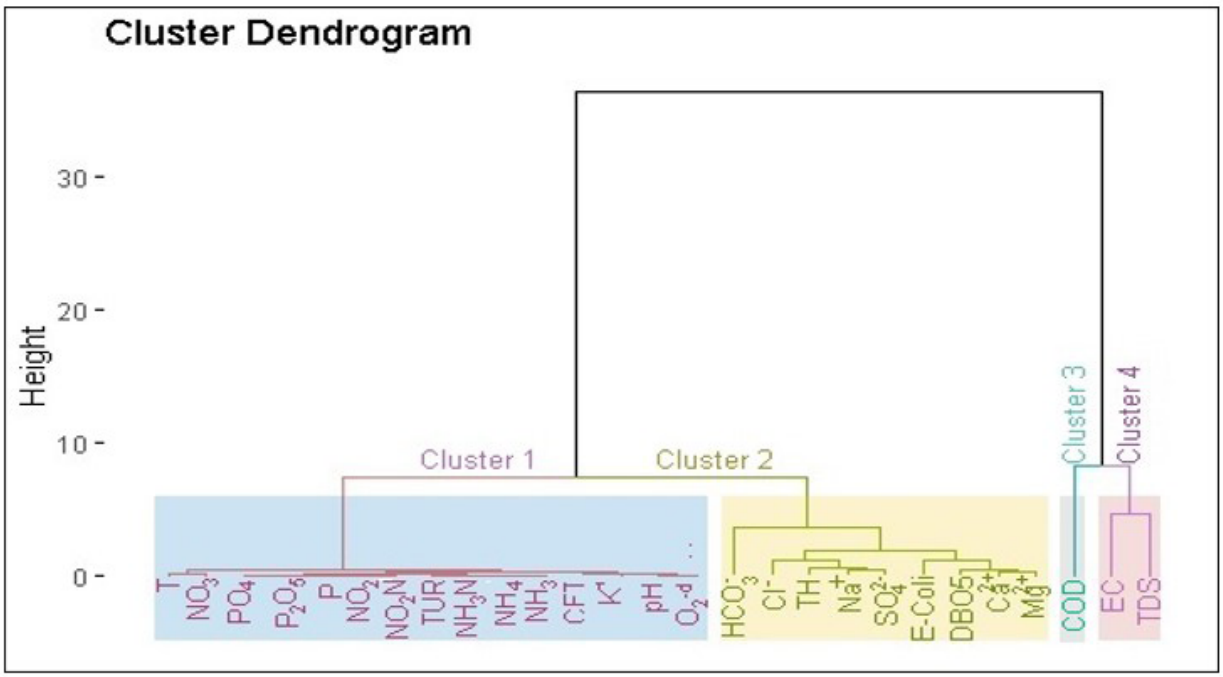

Figure 15. Dendrogram of total physico-chemical and microbiological parameters for the alluvial aquifer.

to criteria related to inertia calculations, the partition obtained by the aggregation of two elements (Bebba, 2017).

The dendrogram (Figure 15) represents the result of the cluster analysis; we distinguish four main families of variables. The first family is grouped (T, NO_3, PO_4, P_2O_5, P, NO_2, NO_2N, TUR, NH_3N, NH_4, NH_3, CFT, K^+, pH and O_2 _d) represented the netrogenous and phosphorus compounds, the groundwater contamination in NO_3^- and P can occur from a variety of sources, including agricultural, urban, and uncontrolled discharges, as well as from the oxidation and/or decomposition of organic waste linked to human activities (Soro et al., 2019), this family is to be related to the diversity of mineralization processes strongly dependent on the pH of water. The seconde family grouping of major ions has a high concentration (Cl^-, SO_4^{2-}, Na^+, Ca^{2+}, and TH) and the presence of E-coli and DBO5 shows that we have two sources of mineralization of these waters; the first is natural from water-rock interactions and residence time in the aquifer, and the second source is due to surface inputs by infiltration of urban

pollutants generated by human activities; the third closer presented by COD. Finally, the fourth one is formed by the parameters CE, TDS, which determine the degree of the waters's mineralization.

CONCLUSION

In conclusion, the study conducted on the hydrochemical quality of the alluvial groundwater of Tebessa reveals a significant influence of wastewater on its characteristics. The investigation utilized hydrochemical methods, geostatistical analysis, graphical representations, and multivariate statistical analysis to assess the hydrogeochemical and microbiological characteristics of the water.

The alluvial aquifer in the region has an average depth of 21 m. The physical properties of the water indicate that the temperature ranges from 13.5 to 20.3 °C, with an average of 17.5 °C. The pH values of the water range from 6.46 to 8.3, with an average of 6.97, suggesting a neutral to alkaline nature. The electrical conductivity varies from medium to high, with values ranging from 701 to 8680 µS.cm-1 and an average of 2745 $\mu S.cm^{-1}$.

Three primary factors were found to influence the mineralization of the water in the region by Principal Component Analysis (PCA) and Cluster Analysis (CA): contact water-rock, residence time or hydrolysis, and precipitation-soils. The hydrochemical properties of the alluvial groundwater are also deteriorating as a result of human activity, such as the generation of waste pollutants. Elevated levels of total coliforms and faecal germs (E-Coli) suggest recent human contamination (Yanko, 2000). Thematic maps of chemical parameters illustrate that the southeastern zone of the study area is more affected, potentially due to the use of wastewater in irrigation and the application of chemical and organic fertilizers in agriculture. The dominant chemical facies in the water include Ca^{2+}-HCO_3^-, mixed Ca^{2+}-Mg-Cl^-, and Ca^{2+}-Cl^-.

Overall, the study highlights the strong influence of anthropogenic activities on the physicochemical and bacteriological quality of both superficial and groundwater in the study area. These findings emphasize the importance of implementing appropriate measures to mitigate the degradation of groundwater and ensure their sustainability.

REFERENCES

Ajaj, Q., Shareef, M., Hassan, N., Hasan, S., & Noori, A. (2018). GIS based spatial modeling to mapping and estimation relative risk of different diseases using Inverse Distance Weighting (IDW) interpolation algorithm and Evidential Belief Function (EBF) (Case study: Minor Part of Kirkuk City, Iraq). *IACSIT International Journal of Engineering and Technology*, *7*(4.37), 185-191. http://doi.org/10.14419/ijet.v7i4.37.24098.

Akoteyon, I. S. (2013). Evaluation of groundwater quality using water quality indices in parts of Lagos-Nigeria. *Journal of Environmental Geography*, *6*(1-2), 29. http://doi.org/10.2478/v10326-012-0004-2.

Alamdar, R., Kumar, V., Moghtaderi, T., & Naghibi, S. J. (2019). Groundwater quality evaluation of Shiraz City, Iran using multivariate and geostatistical techniques. *SN Applied Sciences*, *1*(11), 1367. http://doi.org/10.1007/s42452-019-1108-x.

Annapoorna, H., & Janardhana, M. R. (2015). Assessment of groundwater quality for drinking purpose in rural areas surrounding a defunct copper mine. *Aquatic Procedia*, *4*, 685-692. http://doi.org/10.1016/j.aqpro.2015.02.088.

Bebba, N. (2017). *Impact des paramètres environnementaux et distribution spatio-temporelle des éphéméroptères dans les oueds de biskra et batna* (Doctoral dissertation). Université Ferhat Abbas, Setif.

Brahmi, S., Baali, F., Hadji, R., Brahmi, S., Hamad, A., Rahal, O., Zerrouki, H., Saadali, B., & Hamed, Y. (2021). Assessment of groundwater and soil pollution by leachate using electrical resistivity and induced polarization imaging survey, case of Tebessa municipal landfill, NE Algeria. *Arabian Journal of Geosciences*, *14*(4), 249. http://doi.org/10.1007/s12517-021-06571-z.

Chakraborty, M., Tejankar, A., Coppola, G., & Chakraborty, S. (2022). Assessment of groundwater quality using statistical methods: a case study. *Arabian Journal of Geosciences*, *15*(12), 1136. http://doi.org/10.1007/s12517-022-10276-2.

Chu, J., Song, S., Tan, H., Liu, N., & Liu, F. (2020). Analysis of groundwater pollution caused by mine leachate leakage considering natural impermeable layer. *IOP Conference Series. Earth and Environmental Science*, *585*(1), 012096. http://doi.org/10.1088/1755-1315/585/1/012096.

Diongue, D. M. L., Sagnane, L., Emvoutou, H., Faye, M., Gueye, I. D., & Faye, S. (2022). Evaluation of groundwater quality in the deep maastrichtian aquifer of senegal using multivariate statistics and water quality Index-Based GIS. *Journal of Environmental Protection*, *13*(11), 819. http://doi.org/10.4236/jep.2022.1311052.

Djahadi, S. D., Sandao, I., Ahmed, Y., Harouna, M., & Ousmane, B. (2022). Caractéristiques physico-chimiques des eaux souterraines du socle du bassin versant de Goroubi dans la commune de Torodi /Liptako nigérien. *International Journal of Biological and Chemical Sciences*, *15*(6), 2715. http://doi.org/10.4314/ijbcs.v15i6.35.

Drias, T., & Toubal, A. (2015). Cartographie de la vulnerabilite a la pollution de la nappe alluviale de Tebessa-Morsott (bassin versant de l'oued Ksob) extreme Est Algerien. *LARHYSS Journal*, *12*(2), 35-48.

Drias, T., Khedidja, A., Belloula, M., Saadali, B., Boufekane, A., & Zghibi, A. (2022). *Title Groundwater modelling of the Tebessa-Morsott alluvial aquifer (northeastern Algeria): a geostatistical approach Suggested reviewers*. Retrieved 2023, February 10, from https://www.sciencedirect.com/science/article/abs/pii/S2352801X1930311X

EarthExplorer. (2023). Retrieved 2023, February 10, from https://earthexplorer.usgs.gov/

Fehdi, C., Rouabhia, A., Baali, F., & Boudoukha, A. (2009). The hydrogeochemical characterization of Morsott-El Aouinet aquifer, northeastern Algeria. *Environmental Geology (Berlin)*, *58*(7), 1611-1620. http://doi.org/10.1007/s00254-008-1667-4.

Fehdi, C., Rouabhia, A., Mechai, A., Debabza, M., Abla, K., & Voudouris, K. (2016). Hydrochemical and microbiological quality of groundwater in the Merdja area, Tébessa, North-East of Algeria. *Applied Water Science*, *6*(1), 47-55. http://doi.org/10.1007/s13201-014-0209-3.

Houria, B., Kalla, M., & Zohra, T. F. (2020). Hydrochemical characterisation of groundwater quality: Merdja Plain (Tebessa Town, Algeria). *Civil Engineering Journal*, *6*(2), 318-325. http://doi.org/10.28991/cej-2020-03091473.

Kowalski, W. M., Hamimed, M., & Pharisat, A. (2002). Les etapes d effondrement des grabens dans les confins Algero-Tunisiens. *Bulletin du Service Géologique de l'Algérie*, *13*(2), 131-152.

Lewoyehu, M. (2021). Evaluation of drinking water quality in rural area of Amhara Region, Ethiopia: the case of mecha district. *Journal of Chemistry*, *2021*, e9911838. http://doi.org/10.1155/2021/9911838.

Lloyd, J. W., & Heathcote, J. A. (1985). *Natural inorganic hydrochemistry in relation to groundwater: an introduction*. New York: Clarendon Press.

Mejri, H. E., Moussa, A. B., Salem, S. H., & Zouari, K. (2018). Hydrochemical investigation and quality assessment of groundwater in the BouHafna-Haffouz Unconfined Aquifers, Central Tunisia. In M. Salik Javaid & S. Ali Khan (Eds.), *Aquifers: matrix and fluids*. London: IntechOpen. http://doi.org/10.5772/intechopen.72173.

Mfonka, Z., Ngoupayou, J. N., Ndjigui, P. D., Zammouri, M., Kpoumie, A., & Rasolomanana, E. (2015). Hydrochimie et potabilité des eaux du bassin versant du Nchi dans le plateau Bamoun (Ouest Cameroun). *International Journal of Biological and Chemical Sciences*, *9*(4), 2200. http://doi.org/10.4314/ijbcs.v9i4.39.

Modibo Sidibé, A., Lin, X., & Koné, S. (2019). Assessing groundwater mineralization process, quality, and isotopic recharge origin in the Sahel Region in Africa. *Water*, *11*(4), 789. http://doi.org/10.3390/w11040789.

Moussa, R. S., Alma, M. M. M., Laouli, M. S., Natatou, I., & Habou, I. (2018). Caractérisation physico-chimique des eaux des aquifères du Continental Intercalaire / Hamadien et du Continentalsiems Terminal de la région de Zinder (Niger). *International Journal of Biological and Chemical Sciences*, *12*(5), 5. http://dx.doi.org/10.4314/ijbcs.v12i5.

Moussi, A., & Rebai, N. (2021). A GIS-based tool for automatic extraction of drainage anomalies. A case study of enfidha (North-East of Tunisia). *Geocarto International*, *36*(13), 1533-1547. http://doi.org/10.1080/10106049.2019.1655800.

Naimi-Ait-Aoudia, M., & Berezowska-Azzag, E. (2014). Household water consumption in Algiers facing population growth. In *Water and Cities, Managing a Vital Relationship: 50th ISOCARP Congress 2014*, Gdynia, Poland. Retrieved 2023, February 10, from https://hal.science/hal-01074924/document

Ni, F., Tan, Y., Xu, L., & Fu, C. (2010). DEM and ArcGIS-based extraction of eco-hydrological characteristics in Ya'an, China. In *2010 2nd International Workshop on Intelligent Systems and Applications* (pp. 1-5). New York: IEEE. http://doi.org/10.1109/IWISA.2010.5473679.

Observatory of the Environment in Brittany. (2023). *Nitrogenous matter (excluding nitrates) in Breton rivers: Analysis of annual changes since 1995*. Retrieved 2023, February 10, from https://bretagne--environnement-fr.translate.goog/matieres-azotees-hors-nitrates-cours-eau-bretons-datavisualisation?_x_tr_sl=fr&_x_tr_tl=en&_x_tr_hl=en&_x_tr_pto=sc

Ravikumar, P., Somashekar, R. K., & Prakash, K. (2015). A comparative study on usage of Durov and Piper diagrams to interpret hydrochemical processes in groundwater from SRLIS river basin, Karnataka, India. *Elixir Earth Sci.*, *80*, 31073-31077.

Rodier, J., Legube, B., & Merlet, N. (2009). *L'analyse de l'eau* (9. ed.). Paris: Dunod.

Rouabhia, A., Baali, F., & Fehdi, C. (2009). Impact of agricultural activity and lithology on groundwater quality in the Merdja area, Tebessa, Algeria. *Arabian Journal of Geosciences*, *3*(3), 307-318. http://doi.org/10.1007/s12517-009-0087-4.

Saha, S., Reza, A. H. M. S., & Roy, M. K. (2019). Hydrochemical evaluation of groundwater quality of the Tista floodplain, Rangpur, Bangladesh. *Applied Water Science*, *9*(8), 198. http://doi.org/10.1007/s13201-019-1085-7.

Seghir, K. (2014). La vulnerabilite a la pollution des eaux souterraines de la region Tebessa-Hammamet (Est Algerien). *Larhyss Journal*, *18*, 53-61. Retrieved 2023, February 10, from http://www.larhyss.net/ojs/index.php/larhyss/article/view/204

Semar, A., Saibi, H., & Medjerab, A. (2013). Contribution of multivariate statistical techniques in the hydrochemical evaluation of groundwater from the Ouargla phreatic aquifer in Algeria. *Arabian Journal of Geosciences*, *6*(9), 3427-3436. http://doi.org/10.1007/s12517-012-0616-4.

Singh, A. K., & Kumar, S. R. (2015). Quality assessment of groundwater for drinking and irrigation use in semi-urban area of Tripura, India. *Ecology. Environmental Conservation*, *21*, 97-108.

Soro, G., Soro, T. D., Fossou, N. M.-R., Adjiri, O. A., & Soro, N. (2019). Application des méthodes statistiques multivariées à l'étude hydrochimique des eaux souterraines de la région des lacs (centre de la Côte d'Ivoire). *International Journal of Biological and Chemical Sciences*, *13*(3), 1870. http://doi.org/10.4314/ijbcs.v13i3.54.

Tiwari, A., & Singh, A. (2014). Hydrogeochemical investigation and groundwater quality assessment of Pratapgarh district, Uttar Pradesh. *Journal of the Geological Society of India*, *83*(3), 329-343. http://doi.org/10.1007/s12594-014-0045-y.

Toumi, F., & Alkama, D. (2022). Compatibility between spatial functionalities related to trade with the last administrative organization of Tébessa state–Algeria. *Journal of Al-Azhar University Engineering Sector*, *17*(62), 355-366. http://doi.org/10.21608/auej.2022.216823.

Yanko, W. A. (2000). Of: comparison of Escherichia coli, total coliform, and fecal coliform populations as indicators of wastewater treatment efficiency, G.K. Elmund, M.J. Allen, E.W. Rice. *Water Environment Research*, *72*(2), 253-254. http://doi.org/10.2175/106143000X137455.

Zerhouni, J., Filali, F. R., Bennani, M. N., & Hmaidi, A. E. (2019). Utilisation des systemes d'informations geographiques (SIG) et interpolation pour la caracterisation de la pollution des eaux souterraines en milieu rural de la ville de sebaa ayoune (bassin de sais, maroc). *Journal of Water and Environmental Sciences*, *3*(1), 1.

Authors contributions

Messaoud Abidi Saad: Conception and design, data acquisition, data analysis and interpretation, methodology, software, article writing and content review, and final approval of the version to be published.

Karima Seghir: Conception and design, data acquisition, data analysis and interpretation, methodology, and final approval of the version to be published.

Abdeldjebar Touahri: Conception and design, data acquisition, data analysis and interpretation, methodology, and final approval of the version to be published.

Mehdi Bendekkoum: Data acquisition, data analysis and interpretation, and final approval of the version to be published.

Abdelaziz Bellaoueur: Data acquisition, data analysis and interpretation, and final approval of the version to be published.

Antonio Pulido-Bosch: Methodology, and final approval of the version to be published.